Risk-Averse Strategic Planning of Renewable Energy Grids: A Supply Chain Perspective with Stochastic Supply and Demand

Bo Sun* Pavlo Krokhmal† Yong Chen*

Abstract

This paper considers the problem of strategic long-term planning and operation of energy grids where the power demands are served from renewable energy sources, such as wind farms, and the transmission network is represented by the High-Voltage Direct Current (HVDC) lines. The principal question considered in this work is whether a risk-averse design of the grid, including the selection of wind farm locations and assignment of power delivery from wind farms to customers, would allow for effective hedging of the risks associated with uncertainties in power demands and production of energy from renewable sources.

To this end, the problem is formulated in the general context of supply chain/facility location, with both the supply and the demand being stochastic variates. Several stochastic optimization models are presented and analyzed, including the traditional risk-neutral expectation based model and risk-averse models based on linear and nonlinear coherent measures of risk. Exact solutions algorithms that employ Benders decomposition and polyhedral approximations of nonlinear constraints have been proposed for the obtained linear and nonlinear mixed-integer programming problems. The conducted numerical experiments illustrate the properties of the constructed models, as well as the efficiency of the developed algorithms.

Keywords: Wind farm location, facility location, supply chain, stochastic supply, high-voltage direct current transmission, coherent measures of risk, Benders decomposition, mixed integer p-order cone programming

1 Introduction

The need for effective energy harvesting from renewable resources becomes increasingly important, especially in the light of the inevitable depletion of the fossil fuel energy sources. Among renewable energy sources, wind energy represents one of the most attractive alternatives due to a multitude of factors, including the availability of a relatively mature technology for energy harvesting, a broad range of geographical locations and climates that are suitable for industrial-scale wind power generation, and so on. As a result, the wind energy industry has recently experienced significant worldwide growth. In 2014, the global wind power installed capacity has reached an estimated 336,327 megawatts (MW), which can satisfy around 4% of the world's electricity demand [62].

*Department of Mechanical and Industrial Engineering, University of Iowa, Iowa City, IA 52242, USA

†Department of Systems and Industrial Engineering, University of Arizona, Tucson, AZ 85721, USA, e-mail: krokhmal@email.arizona.edu (corresponding author)

In the United States, the wind energy industry has been one of the fastest growing sectors of economy in the last several years. In 2013, the electricity produced from wind power accounted for 4.13% of all generated electrical energy in the U.S., and became the fifth largest electricity source according to the data from the U.S. Department of Energy's Energy Information Administration (EIA). A technical report from National Renewable Energy Laboratory (NREL) [32] indicates that the United States have the total estimated onshore wind energy potential for 10,955 GW, which could produce 32,784 TWh annually, amounting to almost eight times of total U.S. electricity consumption in 2011. In addition, the offshore wind energy potential is estimated to be 4,150 GW [48]. The U.S. Department of Energy projected that by 2030 wind power could satisfy 20% of total electricity demand in the U.S.

On the other hand, the advantages of wind as a renewable and commonly available source of energy come at a cost of uncertainty in the amount of wind power that can be produced during any given time period. In this respect, power production using renewable energy sources differs drastically from the traditional power production using fossil fuel sources, whose reserves can be accurately estimated and utilized in a controlled manner. As a result, the design and operation of the existing power infrastructure, which implicitly relies on the presumption that power production is completely controllable, may not be ideally suited for the case when a significant portion of generated and consumed power comes from renewable energy sources, such as wind.

In this work, we consider the problem of strategic design and operation of power grids that are based exclusively on wind energy sources, and the primary issue that we aim to elucidate is the problem of effective control of risks of power shortages due to the uncertainties in wind power production and power demands. Specifically, the question of interest is whether risk-averse planning of power grid can be effective for hedging the risks of power shortages due to stochastic variations in power generation and demand.

To this end, we cast the problem of strategic design and operation of renewable energy grid as a *supply chain problem* where both the supply and demand for a specific product (i.e., electric power) are highly stochastic. In particular, we adopt the setting of a stochastic wind farm location model, and employ a class of (generally nonlinear) statistical functionals known as *coherent measures of risk* to quantify and minimize the aforementioned risks of unsatisfied power demand due to uncertainties in power generation are quantified by means of a class of (generally nonlinear) statistical functionals known as *coherent measures of risk* and are minimized through optimal selection of sites for wind energy harvesting and matching of energy producers and customers.

We consider our analysis to be at the *strategic level* as it pertains to planning and operation at the relatively long-term monthly scale with respect to the power generation and demand. The assumption that all power demand within the grid is served by renewable wind energy sources implies that these sources must represent large-scale, massive wind farms. In addition, we assume that the generated electricity is transmitted to demand nodes through high-voltage direct current (HVDC) lines. HVDC transmission lines are used to transmit bulk of electrical energy over long distances by means of direct current (DC), in contrast to the more common alternating current (AC) used in most of today's electrical transmission infrastructure. Since there is no need for reactive compensation along the transmission line, the HVDC lines typically lose less power than equivalent AC transmission lines. This, in addition to lower transmission costs, makes HVDC more economical than AC transmission for large amounts of power transmitted over long distances. Moreover, HVDC transmission can improve system's stability since it allows the operator to quickly change the direction of power flow, as well as allows for the power transportation between power systems with

different frequencies. These characteristics of HVDC transmission make it an appealing choice for renewable energy grids with wind or solar energy sources, as it could aid in mitigating the effects of intermittency and fluctuation and smooth the power outputs, as well as improve the economic viability of renewable energy due to lower transmission costs.

In conclusion of our introductory remarks, we would like to note that the problem setting adopted in this work is more "futuristic" than "realistic", in the sense that industrial-scale power grids where the power is generated entirely from renewable energy sources are unlikely to appear in the foreseeable future. At the same time, we believe that tapping into the idea of building and utilizing a power infrastructure that employs exclusively renewable energy is of scientific and engineering interest, and the present work represents a contribution in this direction. In addition, the obtained results are expected to be of more immediate and practical value in the context of supply chains with stochastic supply and demand.

The remainder of this paper is organized as follows. Section 2 contains a review of relevant literature. In Section 3, we formulate three stochastic wind farm location models with different degrees of risk aversion. Branch-and-bound solution algorithms for the resulting mixed-integer linear and nonlinear programming problems, which employ Benders decomposition method and outer polyhedral approximations of nonlinear constraints, are presented in Section 4. Section 5 discusses dataset generation, computational results, and the corresponding solution analysis.

2 Literature Review

The problem of configuration of power generating systems with renewable energy and storage has been extensively studied. In [50], a genetic algorithm has been proposed to determine the optimal configuration of power system in isolated island with installed renewable energy power plants. Katsigiannis and Georgilakis [26] performed tabu search to solve a combinatorial problem which aimed to optimize sizing of small isolated hybrid power systems. Similarly, Ekren and Ekren [22] applied simulated annealing method for achieving the optimal size of a PV/wind integrated hybrid energy system with battery storage. In addition to these heuristics methods, stochastic programming models have also been employed to design the energy system. Abbey and Joós [1] put forward a stochastic mixed integer programming model to optimize sizing of storage system for an existing isolated wind-diesel power system. In [31], a multi-stage stochastic mixed integer programming model has been presented for a comprehensive hybrid power system design by including renewable energy generation. More particularly, Burke and O'Malley [12] considered the problem which sought to find the optimal locations to incorporate wind capacity on an existing transmission system network. A portfolio approach to optimal wind power deployment in Europe has been studied by Roques et al. [45], who endeavored to smooth out the fluctuations through geographic diversification of wind farms.

This paper considers the strategic-level design and operation of renewable energy power grids in the context of a *supply chain view of the power infrastructure,* and particularly, with respect to the degree to which the power production in the renewable energy grid is capable of meeting the consumers' power demands. From the supply chain point of view, facility location decisions constitute the strategic level of planning [36, 54] and as such represent a crucial factor in reliability and resilience of supply chain operations [34], see also [24, 46, 51].

The key feature of our model is the presence of uncertainties in both demand and supply of electric power. While the literature on strategic facility location and supply chain planning under uncertainties is extensive (see, for example, comprehensive reviews [41, 55] and references therein), majority of the works consider demand-side uncertainty, stochastic costs, travel times, etc.

Here we briefly mention some of the developments most relevant to the present approach. Sheppard [53] presented one of the first scenario-based models of facility location under uncertainties; a stochastic 2-median facility location problem on a probabilistic tree network was first considered in Mirchandani and Oudjit [37]. Weaver and Church [61] and Mirchandani et al. [38] further discussed stochastic versions of p-median location problem and developed solution methods based on Lagrangian relaxation. Louveaux [33] proposed the stochastic versions of the capacitated p-median problem and capacitated fixed-charge location problem with uncertain demands, prices and costs. Berman and Drezner [10] considered a variation of stochastic p-median problem, where additional facilities with knownn probabilities would be located in the future. The α-reliable minimax regret model, which minimized the α-quantile of all regrets was proposed by Daskin et al. [19] . A facility location model which solved for the minimum expected cost while kept relative regret under each scenario limited (p-robust), was formulated by Snyder and Daskin [58]. Chen et al. [15] introduced a model called α-reliable mean-excess regret that instead minimized the expected regret of the "tail" of cost distribution. Robust optimization of a multi-period facility location problem with stochastic demand was discussed in Baron et al. [6].

Literature on supply chain models with stochastic supply is more limited. Among the forms of supply uncertainty that are typically considered, such as supply disruptions, yield uncertainty, capacity uncertainty, and lead time uncertainty (see Snyder et al. [56] for a thorough discussion of these and other aspects), the supply disruptions represent, perhaps, the most commonly discussed factor in supply uncertainties. For example, Drezner [21] considered the supply disruptions for facility location problem by presenting two models, unreliable p-median and (p, q)-center problem where at most q facilities might fail. Reliable versions of p-median and uncapacitated fixed-charge location problem were proposed by Snyder and Daskin [57], which took the expected cost after failures of facilities into consideration. Berman et al. [11] and Shen et al. [52] studied problems similar to [57], but considered heterogeneous disruption probabilities. Also taking account of site-dependent disruption probabilities, Cui et al. [18] studied the reliable uncapacitated fixed-charge location problem through a mixed-integer model and a continuum approximation, respectively. A mixed-integer model for network design with supply disruption, which minimized the nominal cost while bounding the cost with p-robustness, was proposed by Peng et al. [42].

With regard to supply chain models with uncertain demand and supply, Santoso et al. [46] proposed a stochastic programming model for the supply chain network design problem, where the objective function was to minimize the investment and operation costs. Processing/transportation costs, demands, supplies, and capacities were assumed to be stochastic and jointly distributed. Azaron et al. [4] considered a similar model for supply chain design but with multiple objectives, which additionally included the minimization of the variance of the total cost and minimization of the financial risk. A two-stage stochastic program for the supply chain design was formulated by Schütz et al. [47], which involved strategic location decisions in the first stage and operational decisions in the second stage, and where both short-term and long-term uncertainties were considered. Baghalian et al. [5] developed a stochastic model to design a multi-product supply chain network, where supply disruption and demand uncertainty were taken into account simultaneously.

In view of the above, the contributions of the present work can be delineated as follows. In contrast

to aforementioned papers [4, 5, 46, 47], where a penalty multiplier approach was used for to quantify the unsatisfied demand, we employ linear and nonlinear coherent measures of risk to deal with power shortages. In addition, our wind farm location model involves discrete capacity variables at each location, which represent the number of wind turbines to install. From the viewpoint of power grids literature, the present work deals provides one of the relatively few accounts of risk-averse design and operation of power grids, and especially renewable energy grids. Finally, from the computational point of view, this paper furnishes an efficient exact solution method for solving the obtained nonlinear p-order cone mixed integer programming models, which combines the branch-and-bound method based on polyhedral approximations for conic mixed integer problems due to Vielma et al. [59] and Vinel and Krokhmal [60] with Benders decomposition method.

3 Stochastic Wind Farm Location Models

In this section, we introduce several stochastic optimization models that address the problem of strategic location of wind farms so as to satisfy the power demand at a given set of demand sites at a minimum cost. In all models, it is assumed that both the power demand and power generation are uncertain, or stochastic. To model these sources of uncertainty, we adopt the scenario-based approach that is traditional in stochastic programming literature, i.e., we assume that the set of random events Ω in the probability space $(\Omega, \mathcal{F}, \mathsf{P})$ is discrete, $\Omega = \{\omega_1, \ldots, \omega_K\}$, where each elementary random event, or *scenario* ω_k has a non-zero probability $\mathsf{P}\{\omega_k\} = \pi_k > 0$, such that $\sum_k \pi_k = 1$.

Below we present a generic stochastic model (GS) that allows for satisfying the expected demand in each bus (demand node) of the power grid. To this end, we introduce the following notations:

i : index of demand nodes;

j : index of candidate sites of wind farms;

k : index of scenarios;

h : number of wind farms to locate;

γ : cost of power shortages;

λ : annual amortized cost per mile of HVDC transmission line built;

M : an upper bound on the number of wind turbines that can be installed at a given candidate site; for simplicity, it is assumed to be constant across all sites;

f_j : annual amortized fixed cost of wind farm site j;

c_j : annual amortized cost of per turbine purchased and installed at site j;

π_k : probability of scenario k

d_{ij} : distance from node i to candidate site j;

Q_{jk} : power output of a wind turbine in candidate site j under scenario k;

D_{ik} : power demand at node i under scenario k;

$\overline{D}_i$: expected power demand at node i.

Also, we define the following decision variables:

x_j : binary variable indicating whether wind farm site j is selected;

y_{ij} : binary variable indicating whether demand node i is connected to wind farm site j;

ζ_{ij} : number of turbines at wind farm site j serving demand node i;

q_{ijk} : power generated at wind farm site j serving demand node i under scenario k.

3.1 A generic stochastic model for strategic wind farm location

Using the above notations, a generic stochastic model for strategic wind farm location under uncertainties (GS) can be presented in the form of a mixed-integer linear programming problem:

$$\min \quad \sum_j f_j x_j + \sum_i \sum_j c_j \zeta_{ij} + \sum_i \sum_j \lambda d_{ij} y_{ij} \tag{1a}$$

$$\text{s. t.} \quad \sum_j x_j = h, \tag{1b}$$

$$y_{ij} \leq x_j, \qquad \forall i, j, \tag{1c}$$

$$\zeta_{ij} \leq M y_{ij}, \qquad \forall i, j, \tag{1d}$$

$$q_{ijk} \leq Q_{jk} \zeta_{ij}, \qquad \forall i, j, k, \tag{1e}$$

$$\sum_k \pi_k \sum_j q_{ijk} \geq \overline{D}_i, \qquad \forall i, \tag{1f}$$

$$x_j, y_{ij} \in \{0, 1\},\ \zeta_{ij} \in \mathbb{Z}_+,\ q_{ijk} \in \mathbb{R}_+, \qquad \forall i, j, k. \tag{1g}$$

Objective function (1a) represents the cumulative annual cost to be minimized. Constraint (1b) stipulates that exactly h wind farms are to be located. Constraint (1c) states that a demand node i cannot be assigned to a wind farm j unless a wind farm is located at site j. Constraint (1d) limits the number of wind turbines at site j that can be assigned for serving bus i. Constraint (1e) ensures that power supplied by site j to bus i under scenario k does not exceed the total capacity of all wind turbines assigned at site j to serving bus i. Constraint (1f) ensures that the expected power supplied to bus i from all sites does at least meet the expected demand at bus i. Lastly, constraint (1g) determines the values that decision variables take, where $\mathbb{Z}_+$ and $\mathbb{R}_+$ denote the sets of non-negative integer and real numbers, respectively. In what follows, the feasible set defined by constraints (1b)–(1g) is denoted by $\mathcal{P}$.

Remark 1 Note that the wind farm location model (1) does not include the power flow constraints [14, 20], which define the physically feasible distribution of power in an electric grid, and relate the real and the reactive power, the voltage magnitudes and phases (angles) at each bus in the grid. In accordance to the discussion of the goals of this work in Introduction, the stochastic programming formulation (1) models the operation of a renewable energy grid at a long-term scale, where each scenario reflects *averaged* figures of power production and demand over a relatively long time frame (one month in our case study, see Section 5). In contrast, Kirchhoff's Circuit Laws that underlie the power flow constraints are formulated with respect to exact temporal values of currents and voltages in electrical circuits. The purpose of the generic stochastic model (1), as well as the risk-averse models stochastic that are described below and are derived from (1), is to elucidate the operation of a renewable energy electrical grid as a supply chain, where stochastic supply must be used to satisfy stochastic demand. At the same time, since it is assumed that power is distributed in our grid via HVDC transmission lines, the DC power flow constraints reduce to linear constraints, and as such

can be easily incorporated into the formulated models for a study of power distribution in the grid at shorter time scales. The corresponding solutions algorithms, presented in Section 4, will still be applicable.

3.2 Risk-Averse Models for Strategic Wind Farm Location

It is easy to see that the generic stochastic optimization model (1) is prone to substantial power shortages, which may occur in particular scenarios when the power load at bus i and/or the amount of power supplied to this bus deviate from the corresponding average figures. This is a consequence of the well-known properties of stochastic optimization models where constraints are satisfied "on average" [28]. In order to avoid power shortages, one may require that power load at each bus i be satisfied for every scenario $\omega_k \in \Omega$, which can be written as

$$\max_k \left\{ D_{ik} - \sum_j q_{ijk} \right\} \leq 0, \quad \forall i. \tag{2}$$

This method, also known as "robust optimization" approach [27], has been acknowledged in the literature as such that can often lead to overly conservative and exceedingly costly solutions [28]. In addition, enforcing the last constraint does not guarantee shortage-free power distribution in practice, since the scenario data represents only a finite sample from the generally unknown distributions of power demand and wind power production.

In this work, we pursue a risk-averse stochastic optimization approach which is supposed to avoid the potentially large power shortages associated with the expected-value constraint (1f) as well as the high costs associated with the "robust" constraints (2) by explicitly accounting for the *risks* of power shortages.

To quantify the risk of power shortages that may have large magnitudes but very low probabilities of occurring, we employ a class of statistical functional known as *coherent measures of risk* [3], and, more specifically, the well-known Conditional Value-at-Risk (CVaR) measure [44] and its nonlinear generalizations, Higher Moment Coherent Risk (HMCR) measures [29].

Technically, a *risk measure* is a function $\rho : \mathcal{X} \mapsto \mathbb{R}$, where $\mathcal{X}$ is an appropriately defined linear space of $\mathcal{F}$-measurable functions $X : \Omega \mapsto \mathbb{R}$. Further definition of risk measures $\rho(X)$ typically requires specifying whether the larger or smaller realizations of random element X are considered to be "risky". Here we adopt the setup common in engineering literature, where the random variable $X = X(\mathbf{x}, \omega)$ is assumed to represent the cost or loss associated with the decision $\mathbf{x}$, and thus smaller realizations of X are preferred (the alternative assumption, that X represents payoff or reward is prevalent in economics and finance domains).

Then, $\rho(X)$ as defined above is said to be a *coherent* measure of risk [3, 28] if it satisfies the additional properties of *monotonicity*, $\rho(X_1) \leq \rho(X_2)$ for all $X_1 \leq X_2$; *sub-additivity*, $\rho(X_1 + X_2) \leq \rho(X_1) + \rho(X_2)$; *positive homogeneity*, $\rho(\lambda X) = \lambda \rho(X)$ for a constant $\lambda > 0$; and *translation invariance*, $\rho(X + c) = \rho(X) + c$ for any $c \in \mathbb{R}$. The monotonicity property asserts that smaller losses bear less risk. The sub-additivity property in combination with positive homogeneity provides for *convexity* of coherent risk measures, which entails that coherent measures of risk allow for risk reduction via diversification, and, importantly, admit efficient optimization of risk via the methods of convex programming. The translation invariance property allows for efficient risk hedging, see [3] for a detailed discussion.

From this definition, it is easy to see that the risk measure defined as $\rho(X) = \mathsf{E}X$ is coherent. Hence, if one defines the stochastic cost/loss function X as the energy shortage at site i, $X_i(\omega_k) = D_{ik} - \sum_j q_{ijk}$, then constraints (1f) stipulating that power demand at each bus i must be satisfied on average, can equivalently be interpreted as the requirement of non-negative risk of power shortages at each bus i,

$$\rho(X_i) \leq 0, \quad \forall i. \tag{3}$$

Similarly, another trivial instance of coherent measures of risk is represented by the "maximum loss" measure, $\rho(X) = \max X$, which associates the risk of a stochastic loss or cost X with its largest possible realization (it is assumed here that the distribution of X has a bounded support, in the general case the maximization operator in the definition of this risk measure must be replaced with the essential supremum, $\rho(X) = \operatorname{ess\,sup} X$, see, e.g., [28] for details). Then, the conservative-but-costly approach of ensuring that power demands are satisfied at every scenario, embodied by constraints (2), reduces to the risk constraints of the same form (3) where ρ is selected as the maximum loss measure.

In order to find, as we have proposed above, an effective – both methodologically and computationally – compromise between the "loose", risk-neutral expectation-based constraints (1f) and the most conservative risk-averse constraints (2), we will employ the well-known Conditional Value-at-Risk (CVaR) measure [44]. For a given confidence level $\alpha \in (0, 1)$, Conditional Value-at-Risk $\mathsf{CVaR}_\alpha(X)$ can be interpreted as the expected cost or loss that can occur with probability $1-\alpha$ over the prescribed time horizon, or as the average of the $(1-\alpha)\cdot 100\%$ of the largest (worst) realizations of the stochastic loss factor X. This interpretation is reflected in the fact that for a continuously distributed X, $\mathsf{CVaR}_\alpha(X)$ can be represented in the form of conditional expectation

$$\mathsf{CVaR}_\alpha(X) = \mathsf{E}[X \mid X \geq F_X^{-1}(\alpha)], \tag{4}$$

where $F_X(t)$ denotes the cumulative distribution function of X, and $F_X^{-1}(\alpha)$ is the α-quantile of X, or such a deterministic value that can be exceeded by X with probability $1-\alpha$. In financial and risk management literature the α-quantile is also known as the Value-at-Risk at the confidence level α, $\mathsf{VaR}_\alpha(X)$.

In the case of general distributions of X, definition (4) does not apply, in the sense that the corresponding conditional expectation is not guaranteed to have coherence properties [44]. It has been shown in [44] that in the general case $\mathsf{CVaR}_\alpha(X)$ can be represented as a convex combination of $F_\alpha^{-1}(X)$ and the conditional expectation of losses strictly exceeding $F_\alpha^{-1}(X)$, with weight coefficients dependent on both X and α. A more computationally attractive definition of CVaR for general loss distributions presents it as the optimal value of the following unconstrained convex optimization problem [43, 44]:

$$\mathsf{CVaR}_\alpha(X) = \min_\eta \ \eta + (1-\alpha)^{-1}\mathsf{E}(X-\eta)_+, \tag{5}$$

where $X_\pm = \max\{0, \pm X\}$. Besides being a coherent measure of risk, $\mathsf{CVaR}_\alpha(X)$ possesses a number of other properties, such as, for example, continuity with respect to the confidence level α. In the context of the preceding discussion, another notable property of the CVaR measure is that, as a function of the parameter α, it includes both $\rho(X) = \mathsf{E}X$ and $\rho(X) = \operatorname{ess\,sup} X$ as special cases:

$$\lim_{\alpha\to 0} \mathsf{CVaR}_\alpha(X) = \mathsf{E}X, \qquad \lim_{\alpha\to 1} \mathsf{CVaR}_\alpha(X) = \operatorname{ess\,sup} X. \tag{6}$$

Hence, to achieve a balance between the "risk-neutral" approach of ensuring that power shortages do not occur on average, and the "absolute risk-averse" approach requiring that power shortages never occur, one may quantify the risk of power shortages using CVaR measure with an appropriately selected value of confidence level $\alpha \in (0,1)$, whereby the shortage risk would be represented by the average of $(1-\alpha)\cdot 100\%$ largest shortages.

To incorporate the quantification of risks of power shortages in the wind farm location model (1) via the Conditional-Value-at-Risk measure, we define the cost/loss function X as the cumulative power shortage over all buses,

$$X(\omega_k) = \sum_i \left(D_{ik} - \sum_j q_{ijk} \right)_+, \quad \forall k. \tag{7}$$

In order to have an additional degree of flexibility in our model, we include $\mathsf{CVaR}_\alpha(X)$ in the objective of problem (1) with an appropriate weight coefficient $\gamma > 0$, which represents the cost (in millions of dollars) of 1MW of power short:

$$\begin{aligned} \min \quad & \sum_j f_j x_j + \sum_i \sum_j c_j \zeta_{ij} + \sum_i \sum_j \lambda d_{ij} y_{ij} + \gamma \mathsf{CVaR}_\alpha(X) \\ \text{s. t.} \quad & x_j, y_{ij}, \zeta_{ij}, q_{ijk} \in \mathcal{P}, \end{aligned}$$

where X is defined by (7). Note that the cost of shortages in the objective function is non-negative due to the fact that $X(\omega_k) \geq 0$ in (7). By further defining auxiliary variables U_k and η, the risk-averse CVaR-based stochastic model (CVaRS) can be formulated as follows:

$$\min \quad \sum_j f_j x_j + \sum_i \sum_j c_j \zeta_{ij} + \sum_i \sum_j \lambda d_{ij} y_{ij} + \gamma \left(\eta + \frac{1}{1-\alpha} \sum_k \pi_k U_k \right) \tag{8a}$$

$$\text{s. t.} \quad U_k \geq \sum_i \left(D_{ik} - \sum_j q_{ijk} \right)_+ - \eta, \qquad \forall k, \tag{8b}$$

$$U_k \in \mathbb{R}_+, \qquad \forall k, \tag{8c}$$

$$x_j, y_{ij}, \zeta_{ij}, q_{ijk} \in \mathcal{P}. \tag{8d}$$

By means of the Conditional Value-at-Risk measure, the risk-averse formulation (8) accounts for the risk of power shortages as the first moment of the $(1-\alpha)$-tail of the shortages distribution. At the same time, the "risk" as a proxy for "large losses that have a low probability of occurring" is commonly associated in the risk management literature with "heavy tails" of distributions, and the distributions of power shortages are well known to be heavy tailed (see, e.g., [16, 25, 35]). Therefore, it is of interest to take into account higher moments of shortage distribution in assessing the risk of power shortages. This can be accomplished with the help of the family of Higher-Moment Coherent Risk (HMCR) measures [29]. Assuming that the space $\mathcal{X}$ admits a sufficient degree of integrability, i.e., $\mathcal{X} = \mathcal{L}^p(\Omega, \mathcal{F}, \mathsf{P})$ for a given $p \geq 1$, the HMCR measures are defined as

$$\mathsf{HMCR}_{p,\alpha}(X) = \min_{\eta \in \mathbb{R}} \ \eta + (1-\alpha)^{-1} \|(X-\eta)_+\|_p, \quad p \geq 1, \quad \alpha \in (0,1), \tag{9}$$

where $\|X\|_p = (\mathsf{E}|X|^p)^{1/p}$. Obviously, the HMCR family contains CVaR as a special case of $p = 1$.

Similarly to CVaR-based formulation (8), minimization of the total cost that includes the shortage risk cost as expressed by a higher tail moment of shortage distribution is given by the following HMCR-based stochastic optimization (HMCRS) model:

$$\min \quad \sum_j f_j x_j + \sum_i \sum_j c_j \zeta_{ij} + \sum_i \sum_j \lambda d_{ij} y_{ij} + \gamma\big(\eta + (1-\alpha)^{-1} U_0\big) \tag{10a}$$

$$\text{s. t.} \quad q_k^{-1/p} U_k \geq \sum_i \left(D_{ik} - \sum_j q_{ijk} \right)_+ - \eta, \qquad \forall k, \tag{10b}$$

$$U_0 \geq \left(U_1^p + \ldots + U_K^p\right)^{1/p}, \tag{10c}$$

$$t \geq 0; \;\; U_k \geq 0, \qquad \forall k, \tag{10d}$$

$$x_j, y_{ij}, \zeta_{ij}, q_{ijk} \in \mathcal{P}. \tag{10e}$$

The nonlinear inequality (10c) represents a p-order cone constraint, whence formulation (10) represents a mixed-integer p-order cone programming (MIpOCP) problem. The next section discusses the solution methods for the proposed risk-averse stochastic wind farm location models CVaRS (8) and HMCRS (10), as well as their special case, the risk-neutral GS model (1).

4 Benders Decomposition Based Branch-and-Bound Algorithms

4.1 General Formulations

The discussed formulations of GS andf CVaRS models can generally be written as mixed-integer linear programming programming problems of the form

$$\begin{aligned} Z \;=\; \min \quad & \mathbf{a}^\top \mathbf{z} + \mathbf{b}^\top \mathbf{u} \\ \text{s. t.} \quad & \mathbf{A}\mathbf{z} + \mathbf{B}\mathbf{u} \leq \mathbf{c}, \\ & \mathbf{z} \in \mathcal{Z} \subset \mathbb{Z}_+^m, \quad \mathbf{u} \in \mathbb{R}_+^\ell, \end{aligned} \tag{MILP}$$

where $\mathbf{z}$ and $\mathbf{u}$ represent an m-dimensional vector of integer variables and an ℓ-dimensional vector of continuous variables, and $\mathcal{Z}$ is a bounded subset of $\mathbb{Z}_+^m$. Assume that problem MILP is bounded and feasible. Then, it can equivalently be represented as

$$Z \;=\; \min \quad \mathbf{a}^\top \mathbf{z} + t(\mathbf{z}) \tag{11a}$$

$$\text{s. t.} \quad \mathbf{z} \in \mathcal{Z}, \tag{11b}$$

where for any given $\mathbf{z} \in \mathcal{Z}$, function $t(\mathbf{z})$ is defined to be the optimal objective value of the linear programming problem

$$t(\mathbf{z}) \;=\; \min \quad \mathbf{b}^\top \mathbf{u} \tag{12a}$$

$$\text{s. t.} \quad \mathbf{B}\mathbf{u} \leq \mathbf{c} - \mathbf{A}\mathbf{z}, \tag{12b}$$

$$\mathbf{u} \geq \mathbf{0}. \tag{12c}$$

Note that since set $\mathcal{Z} \subset \mathbb{Z}_+^m$ is bounded, the unboundedness of the original problem MILP is associated with that of problem (12). By introducing dual variables $\boldsymbol{\xi}$, we can calculate $t(\mathbf{z})$ through

solving its dual problem, under the assumption of boundedness of problem (12). The dual of problem (12) is

$$\begin{aligned} t(\mathbf{z}) \;=\; \max \quad & (\mathbf{c}-\mathbf{A}\mathbf{z})^{\top}\boldsymbol{\xi} \\ \text{s. t.} \quad & \mathbf{B}^{\top}\boldsymbol{\xi} \leq \mathbf{b}, \\ & \boldsymbol{\xi} \leq \mathbf{0}. \end{aligned} \tag{SMILP}$$

If the feasible region of problem SMILP is empty, then the primal subproblem (12) is either unbounded or infeasible, which implies the unboundedness or infeasibility of the original problem MILP. Otherwise, we can enumerate all extreme points $(\boldsymbol{\xi}_{\mathrm{p}}^{1},\ldots,\boldsymbol{\xi}_{\mathrm{p}}^{I})$, and extreme rays $(\boldsymbol{\xi}_{\mathrm{r}}^{1},\ldots,\boldsymbol{\xi}_{\mathrm{r}}^{J})$ of the feasible region of SMILP, where I and J denote the numbers of extreme points and extreme rays. Therefore, the dual subproblem SMILP can be rewritten as

$$t(\mathbf{z}) = \min \quad t \tag{13a}$$

$$\text{s. t.} \quad (\mathbf{c}-\mathbf{A}\mathbf{z})^{\top}\boldsymbol{\xi}_{\mathrm{r}}^{j} \leq 0, \quad \forall\, j = 1,\ldots,J, \tag{13b}$$

$$(\mathbf{c}-\mathbf{A}\mathbf{z})^{\top}\boldsymbol{\xi}_{\mathrm{p}}^{i} \leq t, \quad \forall i = 1,\ldots,I, \tag{13c}$$

$$t \in \mathbb{R}. \tag{13d}$$

By replacing $t(\mathbf{z})$ in problem (11) with that given by formulation (13), we obtain a reformulation of the original problem MILP:

$$\begin{aligned} \min \quad & \mathbf{a}^{\top}\mathbf{z} + t \\ \text{s. t.} \quad & (\mathbf{c}-\mathbf{A}\mathbf{z})^{\top}\boldsymbol{\xi}_{\mathrm{r}}^{j} \leq 0, \quad \forall\, j = 1,\ldots,J, \\ & (\mathbf{c}-\mathbf{A}\mathbf{z})^{\top}\boldsymbol{\xi}_{\mathrm{p}}^{i} \leq t, \quad \forall i = 1,\ldots,I, \\ & \mathbf{z} \in \mathcal{Z}, \quad t \in \mathbb{R}. \end{aligned} \tag{RMILP}$$

We denote problem RMILP but only with a subset of constraints (13b) and (13c) as problem MMILP, representing the master problem of mixed-integer linear programming problem MILP.

The standard Benders decomposition scheme is then invoked, which consists in solving the "relaxed" problem MMILP (as usual, the procedure is initialized by solving MMILP without any constraints (13b) and (13c) and the variable t in its objective disregarded). If it is unbounded, let $\boldsymbol{\xi}_{\mathrm{r}}^{*}$ be the column vector in which all the corresponding simplex multipliers are negative, after simplex terminates. Therefore, $\boldsymbol{\xi}_{r}^{*}$ is an extreme ray of the feasible region of SMILP, whence a feasibility cut

$$(\mathbf{c}-\mathbf{A}\mathbf{z})^{\top}\boldsymbol{\xi}_{\mathrm{r}}^{*} \leq 0 \tag{14a}$$

is added to MMILP and the problem is thus resolved until an optimal solution $(\mathbf{z}^{*},t^{*})$ of MMILP is obtained. Subsequently, the dual subproblem SMILP is solved for the given $\mathbf{z}^{*}$, and let $\boldsymbol{\xi}_{\mathrm{p}}^{*}$ be the corresponding optimal solution, or an extreme point of its feasible region. If $t(\mathbf{z}^{*}) = (\mathbf{c}-\mathbf{A}\mathbf{z}^{*})^{\top}\boldsymbol{\xi}_{\mathrm{p}}^{*} > t^{*}$, then problem MMILP is augmented with the optimality cut

$$(\mathbf{c}-\mathbf{A}\mathbf{z})^{\top}\boldsymbol{\xi}_{\mathrm{p}}^{*} \leq t \tag{14b}$$

and resolved.

The decomposition procedure stops when the condition $t(\mathbf{z}^*) = t^*$ is satisfied. During each iteration, a feasibility or optimality cut is added, and an optimal solution of RMILP is obtained in a finite number of iterations due to finiteness of I and J [9]. The following two propositions follow readily from the above discussion.

Proposition 1 *If $\tilde{\mathbf{z}} \in \mathcal{Z}$ and there is an optimal solution to the dual subproblem* SMILP *with objective value $\tilde{t} = \max\{(\mathbf{c} - \mathbf{A}\tilde{\mathbf{z}})^\top \boldsymbol{\xi} : \mathbf{B}^\top \boldsymbol{\xi} \leq \mathbf{b}, \boldsymbol{\xi} \leq \mathbf{0}\}$, then $\mathbf{a}^\top \tilde{\mathbf{z}} + \tilde{t}$ is an upper bound on the optimal solution value of problem* RMILP.

Proposition 2 *Assume that $(\mathbf{z}^*, t^*)$ is an optimal solution of the master problem* MMILP. *If the optimal objective value of the corresponding problem* SMILP *is equal to t^*, i.e., $t^* = \max\{(\mathbf{c} - \mathbf{A}\mathbf{z}^*)^\top \boldsymbol{\xi} : \mathbf{B}^\top \boldsymbol{\xi} \leq \mathbf{b}, \boldsymbol{\xi} \leq \mathbf{0}\}$, then $(\mathbf{z}^*, t^*)$ is an optimal solution to the equivalent reformulation of the original problem* RMILP.

4.2 Benders Decomposition Based Algorithm for GS and CVaRS Models

In the following, we denote problems MMILP and RMILP with relaxed integrality constraints (namely, $\mathbf{z} \in \mathcal{Z} \subset \mathbb{Z}_+^m$ replaced by $\mathbf{z} \in \text{conv}(\mathcal{Z}) \subset \mathbb{R}_+^m$) as problem MLP and problem RLP, respectively. Furthermore, we define a node n in the branch-and-bound tree by a triple $(\underline{\mathbf{z}}^n, \bar{\mathbf{z}}^n, \underline{Z}^n) \in \mathbb{Z}_+^{2m} \times (\mathbb{R} \cup \{+\infty\})$, where $(\underline{\mathbf{z}}^n, \bar{\mathbf{z}}^n)$ are the bounds on $\mathbf{z}$ at node n and $\underline{Z}^n$ is a lower bound on $Z_{\text{MLP}(\underline{\mathbf{z}}^n, \bar{\mathbf{z}}^n)}$. The problem $\text{MLP}(\underline{\mathbf{z}}^n, \bar{\mathbf{z}}^n)$ is defined as the problem MLP with added constraints $\underline{\mathbf{z}}^n \leq \mathbf{z} \leq \bar{\mathbf{z}}^n$, and $Z_{\text{MLP}(\underline{\mathbf{z}}^n, \bar{\mathbf{z}}^n)}$ is the corresponding optimal objective value. Similarly, for any $\hat{\mathbf{z}}^n \in \mathbb{Z}_+^m$ we denote by $\text{SMILP}(\hat{\mathbf{z}}^n)$ by replacing the variable $\mathbf{z}$ with the value $\hat{\mathbf{z}}^n$ in problem SMILP, and by $Z_{\text{SMILP}(\hat{\mathbf{z}}^n)}$ the corresponding optimal objective value. In addition, we introduce $\overline{Z}$ and $\mathcal{N}$ to denote the global upper bound on Z_{RMILP} and the set of active branch-and-bound nodes, respectively. The algorithm is described as follows (see **Algorithm 1** for details).

Step 1 Initialize the set of active branch-and-bound nodes $\mathcal{N}$ with root node defined as $(\underline{\mathbf{z}}^0, \bar{\mathbf{z}}^0, \underline{Z}^0)$, and global upper bound $\overline{Z}$ with positive infinity.

Step 2 Select and remove a node from the set $\mathcal{N}$.

Step 3 Solve problem $\text{MLP}(\underline{\mathbf{z}}^n, \bar{\mathbf{z}}^n)$.

Step 4 If the solution of problem $\text{MLP}(\underline{\mathbf{z}}^n, \bar{\mathbf{z}}^n)$ is feasible and its optimal objective value is less than the current global upper bound $\overline{Z}$, go to **Step 5**; otherwise, fathom this node and go to **Step 2**.

Step 5 Denote the optimal solution to problem $\text{MLP}(\underline{\mathbf{z}}^n, \bar{\mathbf{z}}^n)$ by $(\hat{\mathbf{z}}^n, \hat{t}^n)$. If the values of $\hat{\mathbf{z}}^n$ are all integers, go to **Step 6**; otherwise, branch on this node and go to **Step 2**.

Step 6 Solve the problem $\text{SMILP}(\hat{\mathbf{z}}^n)$. If its optimal objective value equal to $\hat{t}^n$ obtained in **Step 5**, then update the global upper bound $\overline{Z}$ and incumbent solution, and fathom this node; otherwise, go to **Step 7**.

Step 7 Check the solution status of problem $\text{SMILP}(\hat{\mathbf{z}}^n)$, if it is unbounded, then add a feasibility cut to problem $\text{MLP}(\underline{\mathbf{z}}^n, \bar{\mathbf{z}}^n)$, go to **Step 3**; otherwise, check whether $Z_{\text{SMILP}(\hat{\mathbf{z}}^n)} > \hat{t}^n$, if it is true, then add an optimality cut to problem $\text{MLP}(\underline{\mathbf{z}}^n, \bar{\mathbf{z}}^n)$, go to **Step 3**.

Algorithm 1 A Benders decomposition based branch-and-bound algorithm for GS and CVaRS models

Set global upper bound $\overline{Z} := +\infty$; set $\underline{Z}^0 := -\infty$
Set $\underline{z}_r^0 := -\infty$, $\bar{z}_r^0 := +\infty$ for all $r \in \{1, \ldots, m\}$; initialize node list $\mathcal{N} := \{(\underline{\mathbf{z}}^0, \bar{\mathbf{z}}^0, \underline{Z}^0)\}$
while $\mathcal{N} \neq \emptyset$ **do**
    Select and remove a node $(\underline{\mathbf{z}}^n, \bar{\mathbf{z}}^n, \underline{Z}^n)$ from $\mathcal{N}$
    Solve $\mathsf{MLP}(\underline{\mathbf{z}}^n, \bar{\mathbf{z}}^n)$
    if $\mathsf{MLP}(\underline{\mathbf{z}}^n, \bar{\mathbf{z}}^n)$ is feasible **and** $Z_{\mathsf{MLP}(\underline{\mathbf{z}}^n, \bar{\mathbf{z}}^n)} < \overline{Z}$ **then**
        Let $(\hat{\mathbf{z}}^n, \hat{t}^n)$ be the optimal solution to $\mathsf{MLP}(\underline{\mathbf{z}}^n, \bar{\mathbf{z}}^n)$
        if $\hat{\mathbf{z}}^n \in \mathbb{Z}_+^m$ **then**
            Solve $\mathsf{SMILP}(\hat{\mathbf{z}}^n)$
            if $Z_{\mathsf{SMILP}(\hat{\mathbf{z}}^n)} = \hat{t}^n$ **then**
                $\overline{Z} := Z_{\mathsf{MLP}(\underline{\mathbf{z}}^n, \bar{\mathbf{z}}^n)}$; update incumbent solution
            else
                if $\mathsf{SMILP}(\hat{\mathbf{z}}^n)$ *is unbounded* **then**
                    Add feasibility cut (14a) to $\mathsf{MLP}(\underline{\mathbf{z}}^n, \bar{\mathbf{z}}^n)$; **go to** 5
                if $Z_{\mathsf{SMILP}(\hat{\mathbf{z}}^n)} > \hat{t}^n$ **then**
                    Add optimality cut (14b) to $\mathsf{MLP}(\underline{\mathbf{z}}^n, \bar{\mathbf{z}}^n)$; **go to** 5
        else
            Select r_0 in $\{r \in \{1, \ldots, m\} : \hat{z}_r^n \notin \mathbb{Z}_+\}$
            Let $\underline{z}_r := \underline{z}_r^n$, $\bar{z}_r := \bar{z}_r^n$ for all $r \in \{1, \ldots, m\} \backslash \{r_0\}$
            Let $\bar{z}_{r_0} := \lfloor \hat{z}_{r_0}^n \rfloor$, $\underline{z}_{r_0} := \lfloor \hat{z}_{r_0}^n \rfloor + 1$
            $\mathcal{N} := \mathcal{N} \cup \left\{ \left(\underline{\mathbf{z}}^n, \bar{\mathbf{z}}, Z_{\mathsf{MLP}(\underline{\mathbf{z}}^n, \bar{\mathbf{z}}^n)}\right), \left(\underline{\mathbf{z}}, \bar{\mathbf{z}}^n, Z_{\mathsf{MLP}(\underline{\mathbf{z}}^n, \bar{\mathbf{z}}^n)}\right) \right\}$
    Remove every node $(\underline{\mathbf{z}}^n, \bar{\mathbf{z}}^n, \underline{Z}^n) \in \mathcal{N}$ such that $\underline{Z}^n \geq \overline{Z}$
end while

Proposition 3 *The Benders decomposition based branch-and-bound algorithm for* GS *and* CVaRS *models terminates with the upper bound* $\overline{Z}$ *equal to the optimal objective value of original problem* MILP.

Proof: The proof is omitted and is analogous to that of the more general Proposition 4 presented in Section 4.3.1. ■

Appendices A.1 and A.2, respectively, present the explicit expressions for the feasibility and optimality cuts that arise in the process of solving the GS and CVaRS models using the described above algorithm.

4.3 HMCRS Model as a Mixed-Integer p-Order Cone Programming Problem

Due to the presence of the p-order cone constraint in formulation (10),

$$U_0 \geq (U_1^p + \ldots + U_K^p)^{1/p}, \tag{15}$$

the HMCRS model represents a mixed-integer p-order cone programming problem (MIpOCP). Below we propose an algorithm for the MIpOCP HMCRS problem that combines the Benders decomposition with a general branch-and-bound algorithm for solving MIpOCP problems that was presented in Vinel and Krokhmal [60]. The idea of the latter method involves solving a polyhedral approximation of the integer relaxation of MIpOCP problem at each node of the BnB tree, and is based on the work of Vielma et al. [59] for mixed integer second order cone programming problems (MISOCP).

Let pOCP denote the integer relaxation of the original MIpOCP problem. Then, a polyhedral approximation of the pOCP relaxation is obtained by replacing nonlinear p-order cone constraints with their polyhedral approximations. It is crucial, however, that such a polyhedral approximation be "compact" with respect to the number of facets, since a straightforward approximation of a p-cone in $\mathbb{R}^{K+1}$ by tangent hyperplanes requires $O(2^K)$ facets. To this end, a *lifted* representation of a multidimensional p-cone is used [8, 60], which expresses a p-cone in $\mathbb{R}_+^{K+1}$ as an intersection of $K-1$ three-dimensional p-cones:

$$U_{2K-1} = U_0, \quad U_{K+k} \geq (U_{2k-1}^p + U_{2k}^p)^{1/p}, \quad k = 1, \ldots, K-1. \tag{16}$$

Then, it is easy to see that if each of the three-dimensional p-cones is replaced by its polyhedral approximation with $O(L)$ facets, the resulting polyhedral approximation of multidimensional p-cone (15) will contain no more than $O(KL)$ facets. In particular, the following gradient-based approximation of three-dimensional p-cones (16) in the positive orthant $\mathbb{R}^3$ was employed in [60]:

$$U_{K+k} \geq a_l^{(p)} U_{2k-1} + b_l^{(p)} U_{2k}, \quad l = 0, \ldots, L, \tag{17a}$$

where

$$a_l^{(p)} = \left(\cos^p \theta_l + \sin^p \theta_l\right)^{\frac{1-p}{p}} \cos^{p-1} \theta_l, \quad b_l^{(p)} = \left(\cos^p \theta_l + \sin^p \theta_l\right)^{\frac{1-p}{p}} \sin^{p-1} \theta_l, \tag{17b}$$

and values θ_l, $l = 0, \ldots, L$, satisfy the condition $0 = \theta_0 < \theta_1 < \ldots < \theta_L = \frac{\pi}{2}$.

The constructed in such a way polyhedral approximation of the pOCP relaxation of the MIpOCP problem is solved instead of the exact nonlinear pOCP formulation at every node of the BnB tree

until an integer-valued solution is found. Since the employed polyhedral approximation is of outer type, its integer solution is not guaranteed to be feasible with respect to the original MIpOCP formulation, whence the exact pOCP relaxation needs to be solved in order to verify feasibility and declare incumbent or branch further (see [60] and [59] for details).

The computational advantages of this approach come from the warm-start capabilities of LP solvers that drastically reduce computational cost of solving a polyhedral approximation of relaxed problem during BnB search in comparison to solving an exact nonlinear relaxation using an interior-point method. The computational overhead associated with the necessity of invoking an exact nonlinear relaxation for testing feasibility of the obtained solution is relatively low. It must be emphasized, however, that the effectiveness of this method is based on the premise that the employed polyhedral approximation is relatively low-dimensional. For example, Vielma et al. [59] used a lifted polyhedral approximation of three-dimensional second-order cones due to Ben-Tal and Nemirovski [8], whose accuracy is exponentially small in the number of facets. The accuracy of gradient approximation (17) of p-cones for $p \neq 2$ is only polynomially small in the number of facets, and a fast cutting plane algorithm was introduced in [30, 60] for solving the resulting polyhedral approximation problems. On the other hand, it has been observed in [59, 60] that the accuracy of polyhedral approximations used during the BnB process may be rather "crude" without a significant deterioration of effectiveness of the algorithm. We use this observation in the present work by employing polyhedral approximation (16)–(17) with a small number L of facets.

Finally, to solve an exact nonlinear relaxation of MIpOCP problem during the BnB algorithm, we use the fact that when $p > 1$ is a rational number, $p = r/s$, a p-order cone in $\mathbb{R}^{K+1}$ can be equivalently represented as a intersection of $O(K \log r)$ three-dimensional second-order cones [7, 39, 40]. Namely, the p-cone (15) is equivalent to

$$U_k^R \leq u_k^s U_0^{r-s} U_k^{R-r}, \quad u_k \geq 0, \qquad k = 1, \ldots, K, \tag{18a}$$

$$U_0 \geq \sum_{k=1}^{K} u_k, \tag{18b}$$

where $R = 2^{\lceil \log_2 r \rceil}$. Then, each nonlinear inequality (18) can be represented by $\lceil \log_2 r \rceil$ three-dimensional "rotated" second-order cones, see [39] for details. For example, in the case of $p = 3$, the p-cone (15) in $\mathbb{R}_+^{K+1}$ admits a representation via $2K$ quadratic cones:

$$U_0 \geq \sum_{k=1}^{K} u_k; \quad U_k^2 \leq U_0 v_k, \;\; v_k^2 \leq u_k U_k, \quad k = 1, \ldots, K.$$

4.3.1 Benders Decomposition Based Branch-and-Bound Algorithm for HMCRS Model

In this section, we propose an efficient method for solving the HMCRS model as a MIpOCP problem that incorporates the Benders decomposition mechanism into the branch-and-bound framework proposed in [59, 60], and as such exploits both the mixed-integer structure of the location problem and p-order cone constraints due to the presence of risk constraints.

By employing the nomenclature introduced in Section 4.1, we represent the HMCRS model (10) in the general form of mixed-integer nonlinear programming problem (MINLP)

$$Z \;=\; \min \quad \mathbf{a}'^{\top}\mathbf{z} + \mathbf{b}'^{\top}\mathbf{u} \tag{MINLP}$$

$$
\begin{aligned}
\text{s. t.} \quad & \mathbf{A}'\mathbf{z} + \mathbf{B}'\mathbf{u} \leq \mathbf{c}', \\
& \mathbf{u} \in \mathcal{K}_p, \\
& \mathbf{z} \in \mathcal{Z} \subset \mathbb{Z}_+^m, \quad \mathbf{u} \geq \mathbf{0},
\end{aligned}
$$

where $\mathcal{K}_p$ is a p-order cone in an appropriate high-dimensional space, such that mixed-integer linear problem MILP is obtained from MINLP by replacing the nonlinear conic constraint with its polyhedral approximation. The integer relaxation of MINLP, obtained by replacing constraint $\mathbf{z} \in \mathcal{Z} \subset \mathbb{Z}_+^m$ by $\mathbf{z} \in \text{conv}(\mathcal{Z}) \subset \mathbb{R}_+^m$, is denoted as NLP. Then, the rest of the definitions stay intact, namely problem RMILP denotes the equivalent Benders reformulation of problem MILP, and MMILP represents the corresponding master problem, or relaxation of RMILP, problem SMILP is the corresponding dual subproblem of MILP, and MLP and RLP stand for problems obtained by relaxing the integrality constraint in problem MMILP and problem RMILP, respectively. Similarly, $\underline{\mathbf{z}}^n$, $\bar{\mathbf{z}}^n$, $\text{MLP}(\underline{\mathbf{z}}^n, \bar{\mathbf{z}}^n)$, $Z_{\text{MLP}(\underline{\mathbf{z}}^n, \bar{\mathbf{z}}^n)}$, $\text{SMILP}(\hat{\mathbf{z}}^n)$, $Z_{\text{SMILP}(\hat{\mathbf{z}}^n)}$ and $\mathcal{N}$ are the same as described in Section 4.2. In addition, we denote the problem obtained by adding constraints $\underline{\mathbf{z}}^n \leq \mathbf{z} \leq \bar{\mathbf{z}}^n$ to problem NLP for any $(\underline{\mathbf{z}}^n, \bar{\mathbf{z}}^n) \in \mathbb{Z}_+^{2m}$ by $\text{NLP}(\underline{\mathbf{z}}^n, \bar{\mathbf{z}}^n)$, and the corresponding optimal objective value by $Z_{\text{NLP}(\underline{\mathbf{z}}^n, \bar{\mathbf{z}}^n)}$. Furthermore, $\underline{Z}^n$ is a lower bound on $Z_{\text{NLP}(\underline{\mathbf{z}}^n, \bar{\mathbf{z}}^n)}$, and $\overline{Z}$ is the global upper bound on Z_{MINLP}. The algorithm is described as follows (see **Algorithm 2** for details).

Step 1-5 The same as described in Section 4.2.

Step 6 Solve the problem $\text{SMILP}(\hat{\mathbf{z}}^n)$. If it is unbounded, then add a feasibility cut to problem $\text{MLP}(\underline{\mathbf{z}}^n, \bar{\mathbf{z}}^n)$ and go to **Step 3**; if its optimal objective value satisfies $Z_{\text{SMILP}(\hat{\mathbf{z}}^n)} > \hat{t}^n$, then add an optimality cut to problem $\text{MLP}(\underline{\mathbf{z}}^n, \bar{\mathbf{z}}^n)$ and go to **Step 3**. If its optimal objective value equal to $\hat{t}^n$ obtained in **Step 5**, go to **Step 7**.

Step 7 Solve problem $\text{NLP}(\hat{\mathbf{z}}^n)$. If it is feasible and its optimal objective value is less than the current global upper bound $\overline{Z}$, then update the global upper bound $\overline{Z}$ and the incumbent solution.

Step 8 If the lower and upper bounds at the current node do not coincide, $\underline{\mathbf{z}}^n \neq \bar{\mathbf{z}}^n$, and $Z_{\text{MLP}(\underline{\mathbf{z}}^n, \bar{\mathbf{z}}^n)} < \overline{Z}$, then solve $\text{NLP}(\underline{\mathbf{z}}^n, \bar{\mathbf{z}}^n)$ and go to **Step 9**; otherwise, fathom this node and go to **Step 2**.

Step 9 If the solution of problem $\text{NLP}(\underline{\mathbf{z}}^n, \bar{\mathbf{z}}^n)$ is feasible and its objective value is less than the current global upper bound $\overline{Z}$, go to **Step 10**; otherwise, fathom this node and go to **Step 2**.

Step 10 Denote the optimal solution to problem $\text{NLP}(\underline{\mathbf{z}}^n, \bar{\mathbf{z}}^n)$ by $(\tilde{\mathbf{z}}^n, \tilde{\mathbf{u}}^n)$. If the values of $\tilde{\mathbf{z}}^n$ are all integers, then update the global upper bound $\overline{Z}$ and incumbent solution, fathom this node and go to **Step 2**; otherwise, branch on this node and go to **Step 2**.

Proposition 4 *The Benders decomposition based branch-and-bound algorithm for* HMCRS *model terminates with the upper bound $\overline{Z}$ equal to the optimal objective value of original problem* MINLP.

Proof: First, since problem MILP is an outer linear approximation of the nonlinear problem MINLP, we may regard MILP as a relaxation of MINLP. Besides, problem MMILP could be deemed as a relaxation of problem MILP because it is a relaxation of problem RMILP, which is an equivalent

Algorithm 2 A Benders decomposition based branch-and-bound algorithm for HMCRS model

Set global upper bound $\overline{Z} := +\infty$; set $\underline{Z}^0 := -\infty$
Set $\underline{z}_r^0 := -\infty$, $\bar{z}_r^0 := +\infty$ for all $r \in \{1, \ldots, m\}$; initialize node list $\mathcal{N} := \left\{\left(\underline{\mathbf{z}}^0, \bar{\mathbf{z}}^0, \underline{Z}^0\right)\right\}$
while $\mathcal{N} \neq \emptyset$ **do**
    Select and remove a node $\left(\underline{\mathbf{z}}^n, \bar{\mathbf{z}}^n, \underline{Z}^n\right) \in \mathcal{N}$
    Solve $\mathsf{MLP}(\underline{\mathbf{z}}^n, \bar{\mathbf{z}}^n)$
    if $\mathsf{MLP}(\underline{\mathbf{z}}^n, \bar{\mathbf{z}}^n)$ is feasible **and** $Z_{\mathsf{MLP}(\underline{\mathbf{z}}^n, \bar{\mathbf{z}}^n)} < \overline{Z}$ **then**
        Let $(\hat{\mathbf{z}}^n, \hat{t}^n)$ be an optimal solution to $\mathsf{MLP}(\underline{\mathbf{z}}^n, \bar{\mathbf{z}}^n)$
        if $\hat{\mathbf{z}}^n \in \mathbb{Z}_+^m$ **then**
            Solve $\mathsf{SMILP}(\hat{\mathbf{z}}^n)$
            if $Z_{\mathsf{SMILP}(\hat{\mathbf{z}}^n)} = \hat{t}^n$ **then**
                Solve $\mathsf{NLP}(\hat{\mathbf{z}}^n)$.
                if $\mathsf{NLP}(\hat{\mathbf{z}}^n)$ is feasible **and** $Z_{\mathsf{NLP}(\hat{\mathbf{z}}^n)} < \overline{Z}$ **then**
                    $\overline{Z} := Z_{\mathsf{NLP}(\hat{\mathbf{z}}^n)}$
                if $\underline{\mathbf{z}}^n \neq \bar{\mathbf{z}}^n$ **and** $Z_{\mathsf{MLP}(\underline{\mathbf{z}}^n, \bar{\mathbf{z}}^n)} < \overline{Z}$ **then**
                    Solve $\mathsf{NLP}(\underline{\mathbf{z}}^n, \bar{\mathbf{z}}^n)$
                    if $\mathsf{NLP}(\underline{\mathbf{z}}^n, \bar{\mathbf{z}}^n)$ is feasible **and** $Z_{\mathsf{NLP}(\underline{\mathbf{z}}^n, \bar{\mathbf{z}}^n)} < \overline{Z}$ **then**
                        Let $(\tilde{\mathbf{z}}^n, \tilde{\mathbf{u}}^n)$ be the optimal solution to $\mathsf{NLP}(\underline{\mathbf{z}}^n, \bar{\mathbf{z}}^n)$
                        if $\tilde{\mathbf{z}}^n \in \mathbb{Z}_+^m$ **then**
                            $\overline{Z} := Z_{\mathsf{NLP}(\underline{\mathbf{z}}^n, \bar{\mathbf{z}}^n)}$
                        else
                            Select r_0 in $\{r \in \{1, \ldots, m\} : \tilde{z}_r^n \notin \mathbb{Z}\}$
                            Let $\underline{z}_r := \underline{z}_r^n$, $\bar{z}_r := \bar{z}_r^n$ for all $r \in \{1, \ldots, m\} \backslash \{r_0\}$
                            Let $\bar{\mathbf{z}}_{r_0} := \lfloor \tilde{z}_{r_0}^n \rfloor$, $\underline{z}_{r_0} := \lfloor \tilde{z}_{r_0}^n \rfloor + 1$
                            $\mathcal{N} := \mathcal{N} \cup \left\{\left(\underline{\mathbf{z}}^n, \bar{\mathbf{z}}, Z_{\mathsf{NLP}(\underline{\mathbf{z}}^n, \bar{\mathbf{z}}^n)}\right), \left(\underline{\mathbf{z}}, \bar{\mathbf{z}}^n, Z_{\mathsf{NLP}(\underline{\mathbf{z}}^n, \bar{\mathbf{z}}^n)}\right)\right\}$
            else
                if $\mathsf{SMILP}(\hat{\mathbf{z}}^n)$ is unbounded **then**
                    Add a feasibility cut (14a) to $\mathsf{MLP}(\underline{\mathbf{z}}^n, \bar{\mathbf{z}}^n)$; **go to** 5
                if $Z_{\mathsf{SMILP}(\hat{\mathbf{z}}^n)} > \hat{t}^n$ **then**
                    Add an optimality cut (14b) to $\mathsf{MLP}(\underline{\mathbf{z}}^n, \bar{\mathbf{z}}^n)$; **go to** 5
        else
            Select r_0 in $\{r \in \{1, \ldots, m\} : \hat{z}_r^n \notin \mathbb{Z}\}$
            Let $\underline{z}_r := \underline{z}_r^n$, $\bar{z}_r = \bar{z}_r^n$ for all $r \in \{1, \ldots, m\} \backslash \{r_0\}$
            Let $\bar{z}_{r_0} := \lfloor \hat{z}_{r_0}^n \rfloor$, $\underline{z}_{r_0} := \lfloor \hat{z}_{r_0}^n \rfloor + 1$
            $\mathcal{N} := \mathcal{N} \cup \left\{\left(\underline{\mathbf{z}}^n, \bar{\mathbf{z}}, Z_{\mathsf{MLP}(\underline{\mathbf{z}}^n, \bar{\mathbf{z}}^n)}\right), \left(\underline{\mathbf{z}}, \bar{\mathbf{z}}^n, Z_{\mathsf{MLP}(\underline{\mathbf{z}}^n, \bar{\mathbf{z}}^n)}\right)\right\}$
    Remove every node $(\underline{\mathbf{z}}^n, \bar{\mathbf{z}}^n, \underline{Z}^n) \in \mathcal{N}$ such that $\underline{Z}^n \geq \overline{Z}$
end while

reformulation of problem MILP. Thus, problem MMILP is a relaxation of problem MINLP, and accordingly problem MLP is a relaxation of problem NLP.

Assuming that the polyhedral relaxation MILP is bounded, this directly implies the finiteness of this algorithm. We may encounter the issue that solution $(\hat{\mathbf{z}}^n, \hat{t}^n)$ is generated again in several nodes if we branch as lines 21–26 in **Algorithm 2**, however, this can only occur a finite number of times, see Vielma et al. [59].

In the following, we will show that an integer feasible solution to problem MINLP that has an objective value strictly less than the cost of the current incumbent integer solution cannot exist in the sub-tree rooted at a fathomed node. Note that a node is only fathomed in lines 6, 15, 17 and 19 in **Algorithm 2**. In line 6, we fathom the node if $\mathsf{MLP}(\underline{\mathbf{z}}^n, \bar{\mathbf{z}}^n)$ is infeasible or if the condition $Z_{\mathsf{MLP}(\underline{\mathbf{z}}^n, \bar{\mathbf{z}}^n)} \geq \overline{Z}$ is satisfied. As it was indicated above, $\mathsf{MLP}(\underline{\mathbf{z}}^n, \bar{\mathbf{z}}^n)$ is a relaxation of $\mathsf{NLP}(\underline{\mathbf{z}}^n, \bar{\mathbf{z}}^n)$, and hence if $\mathsf{MLP}(\underline{\mathbf{z}}^n, \bar{\mathbf{z}}^n)$ is infeasible, $\mathsf{NLP}(\underline{\mathbf{z}}^n, \bar{\mathbf{z}}^n)$ will also be infeasible. In addition, one must have $Z_{\mathsf{NLP}(\underline{\mathbf{z}}^n, \bar{\mathbf{z}}^n)} \geq Z_{\mathsf{MLP}(\underline{\mathbf{z}}^n, \bar{\mathbf{z}}^n)}$. Therefore, an integer feasible solution which is strictly better than the incumbent solution cannot exist in the sub-tree rooted at such a node $(\underline{\mathbf{z}}^n, \bar{\mathbf{z}}^n, \underline{Z}^n)$. Note that in line 10, if $Z_{\mathsf{SMILP}(\hat{\mathbf{z}}^n)} = \hat{t}^n$, then according to Proposition 2, $\hat{\mathbf{z}}$ is in fact an integer feasible solution of problem RMILP, and therefore one has to check problem NLP to make further decision. In line 15, the node is fathomed when $\underline{\mathbf{z}}^n = \bar{\mathbf{z}}^n$ or $Z_{\mathsf{MLP}(\underline{\mathbf{z}}^n, \bar{\mathbf{z}}^n)} \geq \overline{Z}$. If $\underline{\mathbf{z}}^n = \bar{\mathbf{z}}^n$, then $\mathsf{NLP}(\underline{\mathbf{z}}^n, \bar{\mathbf{z}}^n) = \mathsf{NLP}(\hat{\mathbf{z}}^n)$ and hence the node n has been processed by lines 12–14. If $Z_{\mathsf{MLP}(\underline{\mathbf{z}}^n, \bar{\mathbf{z}}^n)} \geq \overline{Z}$, then $Z_{\mathsf{NLP}(\underline{\mathbf{z}}^n, \bar{\mathbf{z}}^n)} \geq \overline{Z}$ since $\mathsf{MLP}(\underline{\mathbf{z}}^n, \bar{\mathbf{z}}^n)$ is a relaxation of $\mathsf{NLP}(\underline{\mathbf{z}}^n, \bar{\mathbf{z}}^n)$. In line 17, the node is fathomed for the same reasons as described above with respect to line 6. The node is fathomed in line 19 because the best integer feasible solution has been found at the sub-tree rooted at the fathomed node. ■

Appendix A.3 furnishes the explicit expressions for the feasibility and optimality cuts that arise in the process of solving the HMCRS model using the described above algorithm.

5 Computational Study

5.1 Parameters and Data

This section provides description and justification for the selected data sets and the particular values of parameters in the three stochastic wind farm location models, GS (1), CVaRS (8), and HMCRS (10) considered in this study.

First, note that the choice of specific values for parameters h (the number of wind farms to locate), p (the order of tail moment in the HMCR measures of risk), and α (the parameter controlling the tail cutoff point in both CVaR and HMCR measures of risk) are at the discretion of the decision maker. It can also be argued that the set of scenario probabilities π_k, $k = 1, \ldots, K$, is in most instances also specified by the decision maker/analyst (e.g., in the case of historic scenario data, one may choose whether to adopt the "physical" probabilities or apply a change of probability measure to work in the domain of "risk-neutral" probabilities, etc).

In the case study reported below, the value of the parameter h is set at $h = 3$, implying that three wind farms are to be established on a given set of candidate locations to serve the demand nodes. The value p in HMCR measure of risk in model (10) is chosen as $p = 3$, and the values of α are selected at $\alpha = 0.95$ for the CVaRS model and $\alpha = 0.90$ for the HMCRS model.

The rest of the parameters can be separated into two categories: deterministic parameters, namely γ, λ, f_j, c_j and d_{ij}, which are assumed to be constant across scenarios, and stochastic parameters, specifically Q_{jk} and D_{ik}, which represent the uncertainties in wind speed and consumer demand, respectively. A detailed description and rationale behind assigning specific values to these parameters follow next.

Deterministic Parameters The value of the parameter γ represents the cost of power shortages, in millions of dollars per MW short. In this study, we select values of γ in the range of 0 to 0.95 with a step of 0.05 to conduct sensitivity analysis of obtained solutions with respect to γ.

We assume that λ, the estimated cost of HVDC line per mile, is 1.5 million dollars. After amortizing it by 30 years, the cost is equal to 0.05 million dollars per mile per year. To evaluate the fixed cost of building a wind farm, f_j, we refer to Kuznia et al. [31], who estimated this value at 280 million dollars. To account for variation of land prices at different locations, we randomly generated the values of parameter f_j from the uniform distribution $U(260, 300)$, and amortized them by 20 years. Next, the cost of purchasing and installing a single wind turbine is reported to be between 1 and 2 million dollars [17]. Therefore, the corresponding costs c_j have been randomly generated from the uniform $U(1, 2)$ distribution (in millions of dollars), and amortized over 20 years. The distances d_{ij} were randomly generated from the uniform $U(200, 2000)$ distribution (in miles); in addition, to model the "extreme" situations when building a transmission line from site j to demand node i is infeasible or prohibitively expensive, some of the distances were randomly set equal to 1,000,000 miles.

Stochastic Parameters The values of parameters Q_{jk} and D_{ik} are obtained either directly from historical data or from Monte Carlo simulation. The corresponding scenario sets are constructed in assumption of equiprobable scenarios, i.e., $\pi_k = 1/K$ for all k; below we discuss the procedures used for scenario generation.

The values of parameter Q_{jk} representing wind turbine power output can be obtained from wind speed data. In this study, the two methods described below were used to generate scenario sets for wind speed (and, consequently, wind power production) distribution. Importantly, we assumed that the wind speed distributions at different site locations are statistically independent.

Historical records of monthly average wind speed data for different locations were obtained through the National Climatic Data Center. Typically, the monthly average wind speed data has a smaller variance and exhibits more symmetry comparing to hourly average wind speed. In this study, we assumed that the average wind speed for each site follows a normal distribution and used maximum likelihood estimation to calculate its mean and standard deviation based on historical monthly average wind speed data. Then, scenario sets for wind speed at different sites were randomly simulated from the estimated normal distributions.

Another commonly used method for simulation of wind speed data relies on Weibull distribution [2, 23], whose probability density function has the form

$$f(x) = \begin{cases} \frac{\kappa}{\xi}\left(\frac{x}{\xi}\right)^{\kappa-1} e^{-(\frac{x}{\xi})^{\kappa}}, & x \geq 0, \\ 0, & x < 0, \end{cases}$$

where κ and ξ are the shape and scale parameters, respectively. To simulate wind speed distribution, the shape parameter of Weibull distribution is often chosen as $\kappa = 2$, and we randomly set the scale parameter as an integer from the range of $8 \leq \xi \leq 14$.

The wind speed data can then be converted to power output Q_{jk} by use of a typical power curve equation [13, 49]

$$P = \frac{1}{2}\rho A v^3 C_{\mathrm{p}},$$

where C_{p} is the power coefficient that is set equal to 0.45, $A = \pi 50^2$ m^2 represents the area swept by the rotor blades of the wind turbine, the density of air ρ is equal to 1.225 kg/m^3, v is the wind speed in m/s. Thus, P is the power output in watts (1 W = 1 kg $\cdot$ m^2/s^3). We then scale the results to MW.

The other stochastic parameter that is considered in this case study is the demand D_{ik} at bus i under scenario k. Similarly to the wind speed data, we also employ two approaches to generating the scenario set for power demand, but, in contrast to wind speed data, we assume that demands at different locations may be correlated.

To construct scenario set for power using historical data, we used the data from Electric Reliability Council of Texas (ERCOT), which describes eight subsection's electricity consumption in the state of Texas, and scaled it by 0.02 in consideration of current wind energy penetration level (around 4%) in the United States.

A second, simulated scenario set was constructed in the assumption that the power demand at each node i follows a mixed normal distribution $XY_1 + (1 - X)Y_2$, where X is a Bernoulli random variable with parameter $\tilde{p}$, and $Y_1 \sim N_1(\mu, \sigma^2)$ and $Y_2 \sim N_2(\mu, 100\sigma^2)$ represent the "normal" demand and "extreme/peak" demand, respectively. The value of parameter $\tilde{p}$ of the Bernoulli distribution was chosen as $\tilde{p} = 0.9$. To account for the correlation between different demand nodes, we consider a correlated multivariate distribution by additionally assuming that distributions N_1 of different nodes are correlated with each other, but N_2 are independent (i.e., one may not expect that occurrence of rare events follows a certain pattern). We use the historical data from Texas to estimate the covariance matrix of demands. The samples of the "extreme" part $N_2(\mu, 100\sigma^2)$ of the mixed normal distribution are independently generated for each node with the σ^2 estimated from the historical data of the state of Texas.

In our numerical experiments, we constructed instances of wind farm location models of two sizes, one with 7 demand nodes and 6 candidate locations, and another with 14 demand nodes and 8 candidate locations. The deterministic parameters for model of each size were generated as described above. For models of each size, the scenario sets for stochastic parameters (the wind power production and power demand) were constructed in two ways, using the historical data and simulated data in accordance to the preceding descriptions.

5.2 Computational Time Comparison

The GS, CVaRS, and HMCRS optimization models, introduced in Section 3, and the corresponding solution algorithms proposed in Section 4 have been implemented in C++ using CPLEX 12.5 solver. In particular, the Benders decomposition-based BnB algorithms described in Sections 4.2–4.3 were implemented using CPLEX's callback functionality, and their computational performance was compared to CPLEX's standard MIP and Barrier MIP solvers. Namely, in the following ta-

bles we denote the standard CPLEX MIP solver as "MIP", and "MIP-B" stands for the Benders decomposition (**Algorithm 1**) algorithm applied to GS and CVaRS models. Similarly, "MISOCP" corresponds to solving the HMCRS model using the default CPLEX MIP Barrier solver as a mixed integer second-order cone programming problem after reformulating the p-order cone constraint via a set of second-order cones [39]. We also denote the cutting-plane based branch-and-bound algorithm for mixed integer p-order cone programming problems due to Vinel and Krokhmal [60] as "BnB", and the Benders decomposition based branch-and-bound algorithm (**Algorithm 2**) as use "BnB-B". The computational experiments were conducted on a 3GHz PC with 4GB RAM running 32-bit Windows 7.

Tables 1, 2, and 3 report the computational performance of the listed algorithms for the risk-neutral (GS), linear risk-averse (CVaRS), and nonlinear risk-averse (HMCRS) problems with varying number of scenarios ($K = 200$, 500, 1000, and 2000), which were generated using either historical or simulated data, for models with either 7 demand nodes and 6 candidate locations or 14 demand nodes and 8 candidate locations.

	GS		CVaRS		HMCRS		
K	MIP	MIP-B	MIP	MIP-B	MISOCP	BnB	BnB-B
200	1.545	0.344	11.295	1.488	6.879	6.639	2.215
500	6.817	1.295	245.968	4.961	31.154	33.011	5.038
1000	40.185	5.242	730.632	13.026	886.495	809.142	20.467

Table 1: Computational time summary (in seconds) for various algorithms applied to GS, CVaRS, and HMCRS problems with scenario sets of K scenarios based on historical data, on a model with 7 demand nodes and 6 candidate locations.

	GS		CVaRS		HMCRS		
K	MIP	MIP-B	MIP	MIP-B	MISOCP	BnB	BnB-B
500	8.097	1.341	60.238	6.396	371.638	118.956	23.000
1000	60.855	5.413	938.591	13.650	906.556	774.880	69.564
2000	284.840	29.156	4061.700	27.144	10803.400	6501.980	217.885

Table 2: Computational time summary (in seconds) for various algorithms applied to GS, CVaRS, and HMCRS problems with scenario sets of K scenarios based on simulated data, on a model with 7 demand nodes and 6 candidate locations.

The conducted computational study indicates that the proposed Benders decomposition allows for drastic reductions in running time for both GS model and CVaRS models as compared to the default CPLEX MIP solver, and the computational improvements tend to increase with the number of scenarios. With regard to the nonlinear HMCRS model, we observe that the "BnB" method that only exploits the structure of p-order cone constraints via polyhedral approximations and the corresponding cutting-plane algorithm, offers relatively mild improvements over "MISOCP", the default CPLEX Barrier MIP solver (which also employs polyhedral approximations). In contrast, the

	GS		CVaRS		HMCRS		
K	MIP	MIP-B	MIP	MIP-B	MISOCP	BnB	BnB-B
100	5.039	3.495	32.749	25.147	55.413	39.564	42.960
200	17.277	2.356	111.346	59.576	409.750	182.297	19.641
500	88.779	7.784	1067.050	113.749	1216.690	922.894	289.238

Table 3: Computational time summary (in seconds) for various algorithms applied to GS, CVaRS, and HMCRS problems with scenario sets of K scenarios based on historical data, on a model with 14 demand nodes and 8 candidate locations.

proposed Benders-based "BnB-B" algorithm significantly outperforms the other two approaches, especially as the number of scenarios increases.

5.3 Out-of-sample solution analysis

In this section, we conduct an out-of-sample analysis of the constructed wind farm location models. To this end, we consider optimal solutions of the risk-neutral and risk-averse problems (GS, CVaRS, and HMCRS, respectively) for given fixed sets of parameters and scenarios, and then compute appropriate quantities of interest (for example, power shortages) under the assumption that one of the relevant parameters of the model assumes values that are different from those used in the corresponding optimization problem (i.e., we "test" the obtained solutions on data samples that were not used during optimization). Importantly, our out-of-sample analysis focuses on the "extreme", or "worst-case" scenarios, in order to emphasize the effects of risk-aversion in the solutions of the proposed models.

5.3.1 Shortage Analysis

Specifically, we assume that the out-of-sample data is represented by power demands D_{ik} (obviously, all parameters in the respective mathematical programming problems can be replaced with out-of-sample values; but for simplicity and clarity of interpretation of the results, in this study the out-of-sample data includes only the power demands).

We analyzed out-of-sample shortages across the grid, $\sum_i (D_{ik} - \sum_j \zeta_{ij} Q_{jk})_+$, induced by the optimal solutions of GS, CVaRS, and HMCRS problems in the case of a model with demand 7 nodes and 6 candidate locations and 2000 scenarios based on simulated data, as well as in the case of 14 demand nodes and 8 candidate locations, both with value of parameter $\gamma = 0.24$. We randomly generated a dataset consisting of 2000 scenarios of consumer demand D_{ik} from the same mixed normal distribution, and selected the scenarios with shortages beyond 0.95 sample quantile in our out-of-sample scenario set as the "extreme", or "worst-case" scenarios (in other words, the out-of-sample scenario set contained a total of 100 scenarios that represent 5% of highest power shortage levels).

The results are presented in the shortage histograms and boxplots in Figures 1 and 2. In the case of the smaller model with 7 demand nodes and 6 candidate locations, the boxplots of shortages

indicate that both risk-averse models, HMCRS and CVaRS, significantly outperform the risk-neutral GS model. The CVaRS model has smaller 0.75 quantile value of shortages than HMCRS model, but it has larger extreme points. This observation is in accord with γ sensitivity analysis presented in the next section. Analysis of shortage histograms shows that all shortages for HMCRS model are within 500 MW, and most of its shortages fall in the range of [0, 50) MW, while the fraction of zero shortages exceeds 30%. As regards the CVaRS model, shortage has exceeded 500 MW in one scenario, but most of its shortages do not exceed 250 MW, also with a high fraction of zero shortages. In contrast, "extreme" out-of-sample power shortages in GS model are always non-zero and fall mainly between 500 MW and 1000 MW, and can be as high as 1500 MW.

Similarly, in the case of models with 14 demand nodes and 8 candidate locations, boxplots in Figure 2 indicate that the HMCRS model has the lowest 0.25 quantile, median, 0.75 quantile, etc., and CVaRS model performs much better than the GS model. The histograms of power shortages indicate that over 20% of out-of-sample shortages are within $[0, 250)$ MW for HMCRS model. However, no shortages fall into this range in the case of CVaRS and GS models. Also, 98% of "extreme" out-of-sample shortages are below 1000 MW for HMCRS model. Although over 70% of "extreme" out-of-sample shortages are under 1000 MW for CVaRS model, there is a substantial number of out-of-sample shortages within [1000,1500) MW, and even reaching 2000 MW in one scenario. As regards the GS model, most of its shortages are between 1000 MW and 2000 MW, and it has nearly 5% of "extreme" out-of-sample shortages beyond 2000 MW. The largest shortage that was observed in the GS model is close to 2500 MW.

5.3.2 Sensitivity with Respect to Shortage Penalty Parameter γ

Recall that the sensitivity to power shortages of the risk-averse CVaRS and HMCRS models is determined by the parameter γ, which represents the dollar cost of 1 MW of power short. The risk-neutral GS model is insensitive to (does not contain) the parameter γ, and, moreover, for the value of $\gamma = 0$, all three models yield the same solutions. In this section, we evaluate several aspects of the performance of the GS, CVaRS, and HMCRS models with respect to different levels of sensitivity to power shortages, corresponding to varying the value of the parameter γ from 0 to 0.95. Obviously, the solution of the GS model would not change with γ, and can be considered as the "reference" point in this comparison.

To evaluate the performance of three models, we consider four criteria: (1) the amortized annual cost, (2) the mean cumulative shortage across the grid, (3) the number of shortage scenarios, i.e., the scenarios under which shortages occur, and (4) the mean number of demand nodes that experience shortages. The annual cost is computed as $\sum_j f_j x_j + \sum_i \sum_j c_j \zeta_{ij} + \sum_i \sum_j \lambda d_{ij} y_{ij}$; according to Section 5.3, the cumulative shortage at scenario k is defined as $\sum_i (D_{ik} - \sum_j \zeta_{ij} Q_{jk})_+$, and thus mean shortage is $\mathsf{E}[\sum_i (D_{ik} - \sum_j \zeta_{ij} Q_{jk})_+]$. As in the previous section, the out-of-sample analysis is conducted, in the sense that all the four criteria are evaluated on the set of 100 "extreme" out-of-sample scenarios determined as described above, e.g., the mean shortage and the mean number of demand nodes with shortages should be interpreted as a conditional expectations. The four criteria are thus computed for the case of 7 demand nodes and 6 candidate locations and 2,000 scenarios, and values of γ varying from 0 to 0.95 with a step of 0.05. The results are presented in Figure 3, where the horizontal (constant) lines correspond to the GS model.

As expected, the annual costs of CVaRS and HMCRS models increase with γ. In contrast, mean shortage and mean number of shortage nodes in the CVaRS and HMCRS models decrease sharply

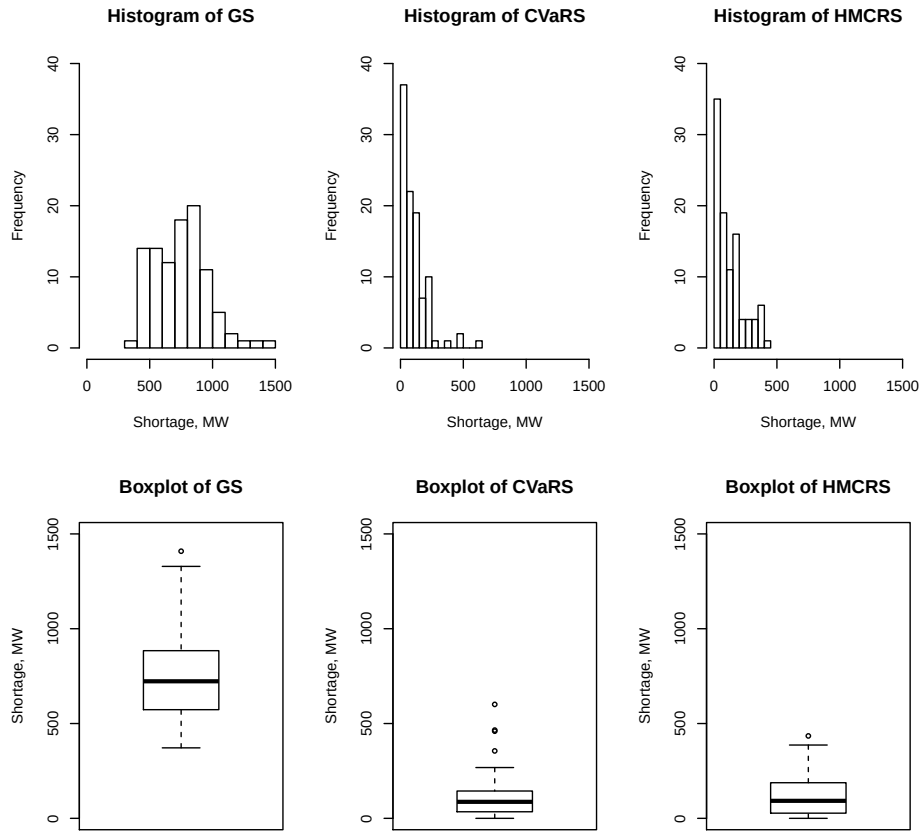

Figure 1: Shortages in out-of-sample extreme scenarios for model with 7 nodes and 6 locations

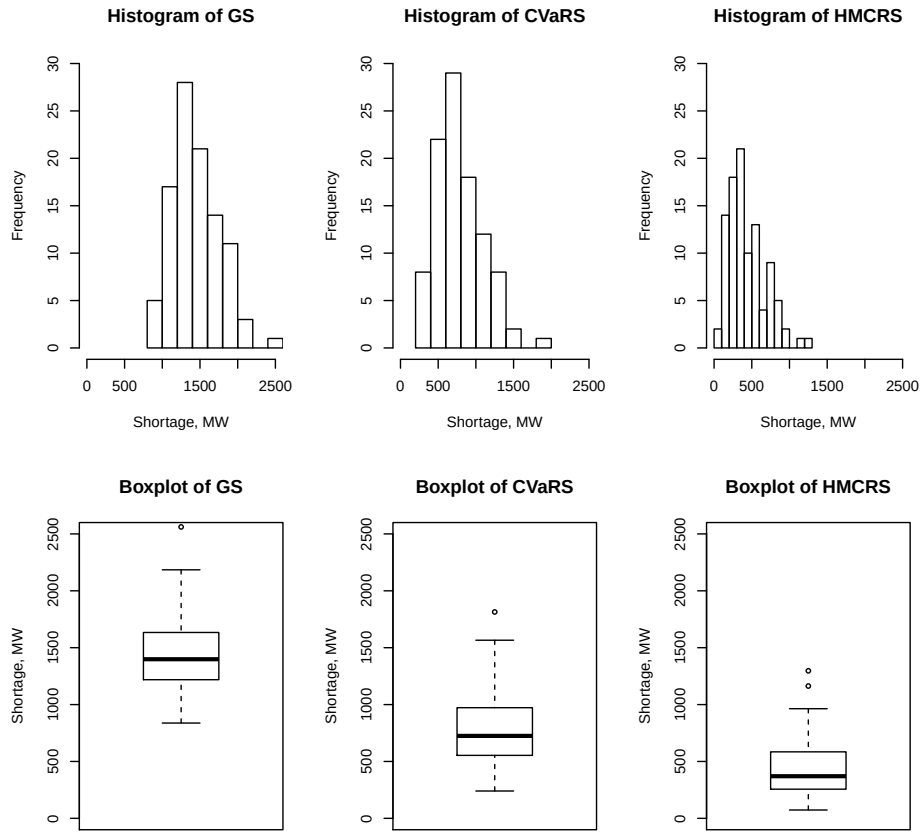

Figure 2: Shortages in out-of-sample extreme scenarios for model with 14 nodes and 8 locations

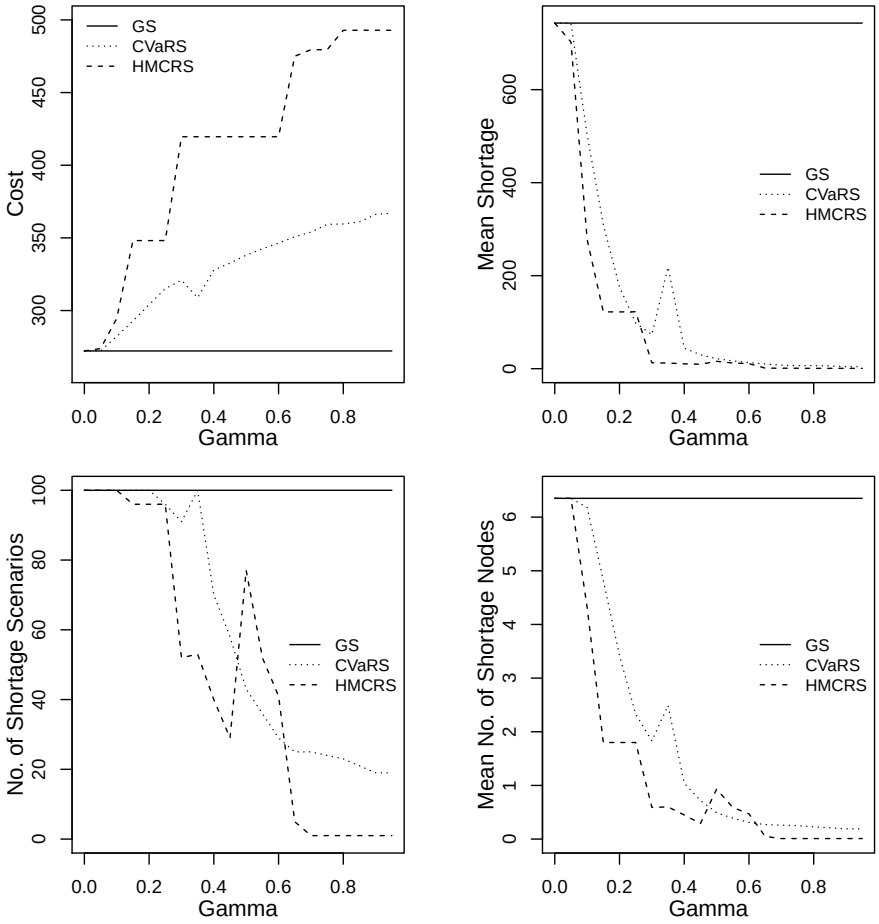

Figure 3: Out-of-sample performance of GS, CVaRS and HMCRS with regard to γ

with γ. Compared with the CVaRS model, the HMCRS model always performs better in terms of criteria (2)–(4), except for values γ around 0.5, but incurs higher annual costs. In conclusion, CVaRS and HMCRS models could be tuned to fit user's risk-averse preference so as to achieve better risk control of power shortages.

6 Conclusions

In this paper, we have considered three different stochastic optimization models for strategic wind farm location and operation: a risk-neutral model, a two models where risk preferences are represented by a linear risk measure (Conditional Value-at-Risk), and a nonlinear risk measure (Higher-Moment Coherent Risk measure). We proposed a branch-and-bound algorithm based on Benders decomposition technique to solve the resulting linear and p-order cone mixed-integer programming problems. The conducted numerical study demonstrates the efficiency of developed algorithms, and also indicates the risk-averse models allow for drastic reduction of wind power shortages, and can effectively be used in strategic location and planning problems.

Acknowledgments

This work was supported in part by the NSF grant DMI 0457473 and DTRA grant HDTRA1-14-1-0065.

References

[1] Abbey, C. and Joós, G. (2009) "A stochastic optimization approach to rating of energy storage systems in wind-diesel isolated grids," *Power Systems, IEEE Transactions on*, **24** (1), 418–426.

[2] Aksoy, H., Toprak, Z. F., Aytek, A., and Ünal, N. E. (2004) "Stochastic generation of hourly mean wind speed data," *Renewable energy*, **29** (14), 2111–2131.

[3] Artzner, P., Delbaen, F., Eber, J.-M., and Heath, D. (1999) "Coherent measures of risk," *Mathematical finance*, **9** (3), 203–228.

[4] Azaron, A., Brown, K., Tarim, S., and Modarres, M. (2008) "A multi-objective stochastic programming approach for supply chain design considering risk," *International Journal of Production Economics*, **116** (1), 129–138.

[5] Baghalian, A., Rezapour, S., and Farahani, R. Z. (2013) "Robust supply chain network design with service level against disruptions and demand uncertainties: A real-life case," *European Journal of Operational Research*, **227** (1), 199–215.

[6] Baron, O., Milner, J., and Naseraldin, H. (2011) "Facility location: A robust optimization approach," *Production and Operations Management*, **20** (5), 772–785.

[7] Ben-Tal, A. and Nemirovski, A. (2001) *Lectures on modern convex optimization: analysis, algorithms, and engineering applications*, volume 2 of *MPS/SIAM Series on Optimization*, SIAM.

[8] Ben-Tal, A. and Nemirovski, A. (2001) "On polyhedral approximations of the second-order cone," *Mathematics of Operations Research*, **26** (2), 193–205.

[9] Benders, J. F. (1962) "Partitioning procedures for solving mixed-variables programming problems," *Numerische mathematik*, **4** (1), 238–252.

[10] Berman, O. and Drezner, Z. (2008) "The p-median problem under uncertainty," *European Journal of Operational Research*, **189** (1), 19–30.

[11] Berman, O., Krass, D., and Menezes, M. B. (2007) "Facility reliability issues in network p-median problems: strategic centralization and co-location effects," *Operations Research*, **55** (2), 332–350.

[12] Burke, D. J. and O'Malley, M. (2008) "Optimal wind power location on transmission systems-a probabilistic load flow approach," in: "Probabilistic Methods Applied to Power Systems, 2008. PMAPS'08. Proceedings of the 10th International Conference on," 1–8, IEEE.

[13] Burton, T., Jenkins, N., Sharpe, D., and Bossanyi, E. (2011) *Wind energy handbook*, John Wiley & Sons.

[14] Carpentier, J. (1962) "Contribution a letude du dispatching economique," *Bulletin de la Societe Francaise des Electriciens*, **3** (1), 431–447.

[15] Chen, G., Daskin, M. S., Shen, Z.-J. M., and Uryasev, S. (2006) "The α-reliable mean-excess regret model for stochastic facility location modeling," *Naval Research Logistics (NRL)*, **53** (7), 617–626.

[16] Clauset, A., Shalizi, C. R., and Newman, M. E. (2009) "Power-law distributions in empirical data," *SIAM review*, **51** (4), 661–703.

[17] Conserve Energy Future (2013) "Cost of Wind Energy," `http://www.conserve-energy-future.com/WindEnergyCost.php`, [Online; accessed 12-Nov-2013].

[18] Cui, T., Ouyang, Y., and Shen, Z.-J. M. (2010) "Reliable facility location design under the risk of disruptions," *Operations Research*, **58** (4-part-1), 998–1011.

[19] Daskin, M. S., Hesse, S. M., and Revelle, C. S. (1997) "α-reliable p-minimax regret: A new model for strategic facility location modeling," *Location Science*, **5** (4), 227–246.

[20] Dommel, H. W. and Tinney, W. F. (1968) "Optimal power flow solutions," *IEEE transactions on power apparatus and systems*, (10), 1866–1876.

[21] Drezner, Z. (1987) "Heuristic solution methods for two location problems with unreliable facilities," *Journal of the Operational Research Society*, 509–514.

[22] Ekren, O. and Ekren, B. Y. (2010) "Size optimization of a PV/wind hybrid energy conversion system with battery storage using simulated annealing," *Applied Energy*, **87** (2), 592–598.

[23] Garcia, A., Torres, J., Prieto, E., and De Francisco, A. (1998) "Fitting wind speed distributions: a case study," *Solar Energy*, **62** (2), 139–144.

[24] Ghiani, G., Laporte, G., and Musmanno, R. (2004) *Introduction to logistics systems planning and control*, John Wiley & Sons, New York.

[25] Glass, R., Beyeler, W., Stamber, K., Glass, L., LaViolette, R., Conrad, S., Brodsky, N., Brown, T., Scholand, A., and Ehlen, M. (2005) "Simulation and Analysis of Cascading Failure in Critical Infrastructure," *Technical report*, Sandia National Laboratories.

[26] Katsigiannis, Y. and Georgilakis, P. (2008) "Optimal sizing of small isolated hybrid power systems using tabu search," *Journal of Optoelectronics and Advanced Materials*, **10** (5), 1241.

[27] Kouvelis, P. and Yu, G. (1997) *Robust discrete optimization and its applications*, Kluwer Academic Publishers, Dordrecht.

[28] Krokhmal, P., Zabarankin, M., and Uryasev, S. (2011) "Modeling and optimization of risk," *Surveys in Operations Research and Management Science*, **16** (2), 49–66.

[29] Krokhmal, P. A. (2007) "Higher moment coherent risk measures," *Quantitative Finance*, **7** (4), 373–387.

[30] Krokhmal, P. A. and Soberanis, P. (2010) "Risk optimization with p-order conic constraints: A linear programming approach," *European Journal of Operational Research*, **201** (3), 653–671.

[31] Kuznia, L., Zeng, B., Centeno, G., and Miao, Z. (2011) "Stochastic optimization for power system configuration with renewable energy in remote areas," *Annals of Operations Research*, 1–22.

[32] Lopez, A., Roberts, B., Heimiller, D., Blair, N., and Porro, G. (2012) "U.S. renewable energy technical potentials: a GIS-based analysis," *Technical report*, National Renewable Energy Laboratory.

[33] Louveaux, F. (1986) "Discrete stochastic location models," *Annals of Operations research*, **6** (2), 21–34.

[34] Lu, M., Ran, L., and Shen, Z.-J. M. (2015) "Reliable Facility Location Design Under Uncertain Correlated Disruptions," *Manufacturing & Service Operations Management*, **17** (4), 445–455.

[35] Mei, S., Zhang, X., and Cao, M. (2011) *Power grid complexity*, Springer.

[36] Melo, M. T., Nickel, S., and Saldanha-Da-Gama, F. (2009) "Facility location and supply chain management–A review," *European journal of operational research*, **196** (2), 401–412.

[37] Mirchandani, P. B. and Oudjit, A. (1980) "Localizing 2-medians on probabilistic and deterministic tree networks," *Networks*, **10** (4), 329–350.

[38] Mirchandani, P. B., Oudjit, A., and Wong, R. T. (1985) "'Multidimensional' extensions and a nested dual approach for the m-median problem," *European Journal of Operational Research*, **21** (1), 121–137.

[39] Morenko, Y., Vinel, A., Yu, Z., and Krokhmal, P. (2013) "On p-cone linear discrimination," *European Journal of Operational Research*, **231**, 784–789.

[40] Nesterov, Y., Nemirovskii, A., and Ye, Y. (1994) *Interior-point polynomial algorithms in convex programming*, volume 13 of *Studies in Applied Mathematics*, SIAM, Philadelphia, PA.

[41] Owen, S. H. and Daskin, M. S. (1998) "Strategic facility location: A review," *European Journal of Operational Research*, **111** (3), 423–447.

[42] Peng, P., Snyder, L. V., Lim, A., and Liu, Z. (2011) "Reliable logistics networks design with facility disruptions," *Transportation Research Part B: Methodological*, **45** (8), 1190–1211.

[43] Rockafellar, R. T. and Uryasev, S. (2000) "Optimization of conditional value-at-risk," *Journal of risk*, **2**, 21–42.

[44] Rockafellar, R. T. and Uryasev, S. (2002) "Conditional value-at-risk for general loss distributions," *Journal of Banking & Finance*, **26** (7), 1443–1471.

[45] Roques, F., Hiroux, C., and Saguan, M. (2010) "Optimal wind power deployment in Europea portfolio approach," *Energy Policy*, **38** (7), 3245–3256.

[46] Santoso, T., Ahmed, S., Goetschalckx, M., and Shapiro, A. (2005) "A stochastic programming approach for supply chain network design under uncertainty," *European Journal of Operational Research*, **167** (1), 96–115.

[47] Schütz, P., Tomasgard, A., and Ahmed, S. (2009) "Supply chain design under uncertainty using sample average approximation and dual decomposition," *European Journal of Operational Research*, **199** (2), 409–419.

[48] Schwartz, M., Heimiller, D., Haymes, S., and Walt, M. (2010) "Assessment of offshore wind energy resources for the United States," *Technical report*, National Renewable Energy Laboratory.

[49] Scott, W. R. and Powell, W. B. (2012) "Approximate dynamic programming for energy storage with new results on instrumental variables and projected Bellman errors," *Submitted to Operations Research (Under Review)*.

[50] Senjyu, T., Hayashi, D., Yona, A., Urasaki, N., and Funabashi, T. (2007) "Optimal configuration of power generating systems in isolated island with renewable energy," *Renewable Energy*, **32** (11), 1917–1933.

[51] Shapiro, J. F. (2001) *Modeling the Supply Chain*, Duxbury Press, Pacific Grove, CA.

[52] Shen, Z.-J. M., Zhan, R. L., and Zhang, J. (2011) "The reliable facility location problem: Formulations, heuristics, and approximation algorithms," *INFORMS Journal on Computing*, **23** (3), 470–482.

[53] Sheppard, E. (1974) "A conceptual framework for dynamic location-allocation analysis," *Environment and Planning A*, **6** (5), 547–564.

[54] Simchi-Levi, D., Kaminsky, P., and Simchi-Levi, E. (2004) *Managing the Supply Chain: The Definitive Guide for the Supply Chain Professional*, McGraw-Hill, New York.

[55] Snyder, L. V. (2006) "Facility location under uncertainty: a review," *IIE Transactions*, **38** (7), 547–564.

[56] Snyder, L. V., Atan, Z., Peng, P., Rong, Y., Schmitt, A. J., and Sinsoysal, B. (2015) "OR/MS models for supply chain disruptions: A review," *IIE Transactions*, 1–21.

[57] Snyder, L. V. and Daskin, M. S. (2005) "Reliability models for facility location: the expected failure cost case," *Transportation Science*, **39** (3), 400–416.

[58] Snyder, L. V. and Daskin, M. S. (2006) "Stochastic p-robust location problems," *IIE Transactions*, **38** (11), 971–985.

[59] Vielma, J. P., Ahmed, S., and Nemhauser, G. L. (2008) "A lifted linear programming branch-and-bound algorithm for mixed-integer conic quadratic programs," *INFORMS Journal on Computing*, **20** (3), 438–450.

[60] Vinel, A. and Krokhmal, P. (2014) "Polyhedral approximations in p-order cone programming," *Optimization Methods & Software*, **29** (6), 1210–1237.

[61] Weaver, J. R. and Church, R. L. (1983) "Computational procedures for location problems on stochastic networks," *Transportation Science*, **17** (2), 168–180.

[62] World Wind Energy Association (2014) "2014 Half-year Report," *Technical report*, World Wind Energy Association.

A Feasibility and Optimality Cuts

A.1 Feasibility Cuts for GS Model

The generic stochastic model GS (1) can be written in the form of problem MILP, where the integer-valued vector $\mathbf{z}$ contains variables x_j, y_{ij}, and ζ_{ij}, and nonnegative vector $\mathbf{u}$ contains variables p_{ijk}. Then, the corresponding problem (11) has the form

$$Z \;=\; \min \quad \sum_j f_j x_j + \sum_i \sum_j c_j \zeta_{ij} + \sum_i \sum_j \lambda d_{ij} y_{ij} \tag{19a}$$

$$\text{s. t.} \quad \sum_j x_j = h, \tag{19b}$$

$$y_{ij} \le x_j, \qquad \forall i, j, \tag{19c}$$

$$\zeta_{ij} \le M y_{ij}, \qquad \forall i, j, \tag{19d}$$

$$x_j, y_{ij} \in \{0,1\},\ \zeta_{ij} \in \mathbb{Z}_+, \qquad \forall i, j, k, \tag{19e}$$

where the function $t(\mathbf{z})$ defined as the optimal objective of subproblem (12) is equal to either 0 when the problem

$$t(\mathbf{z}) \ = \ \min \quad 0 \tag{20a}$$

$$\text{s. t.} \quad q_{ijk} \le Q_{jk}\zeta_{ij}, \qquad \forall i, j, k, \tag{20b}$$

$$\sum_k \pi_k \sum_j q_{ijk} \ge \overline{D}_i, \qquad \forall i, \tag{20c}$$

$$q_{ijk} \ge 0, \tag{20d}$$

is feasible for the given values of ζ_{ij}, or $t(\mathbf{z}) = +\infty$ when (20) is infeasible. Obviously, if $\hat{\mathbf{z}} = (\hat{x}_j, \hat{y}_{ij}, \hat{\zeta}_{ij})$ is an optimal solution of (19) such that (20) has a feasible $\hat{q}_{ijk}$ for the given $\hat{\zeta}_{ij}$, then $(\hat{\mathbf{z}}, \hat{\mathbf{u}}) = (\hat{x}_j, \hat{y}_{ij}, \hat{\zeta}_{ij}, \hat{q}_{ijk})$ is an optimal solution of the original problem (1). On the other hand, if (20) is infeasible, then the corresponding $\hat{\mathbf{z}}$ should be eliminated from the feasible region of the master problem (19). In accordance to the described above algorithm, this is accomplished by augmenting (19) with feasibility cuts

$$\sum_i \sum_j \sum_k Q_{jk}\hat{\alpha}_{ijk}\zeta_{ij} - \sum_i \overline{D}_i \hat{\beta}_i \le 0, \tag{21}$$

where $(\hat{\alpha}_{ijk}, \hat{\beta}_i)$ is an extreme ray of the dual $\mathsf{SMILP}(\hat{\mathbf{z}})$ of problem (20), which takes the form

$$t(\hat{\mathbf{z}}) = \max \quad \sum_i \sum_j \sum_k Q_{jk}\hat{\zeta}_{ij}\alpha_{ijk} - \sum_i \overline{D}_i \beta_i \tag{22a}$$

$$\text{s. t.} \quad \alpha_{ijk} - \pi_k \beta_i \le 0, \qquad \forall i, j, k, \tag{22b}$$

$$\alpha_{ijk}, \beta_i \le 0, \qquad \forall i, j, k. \tag{22c}$$

Clearly, no optimality cuts are added to (19) since (20) is a "feasibility" subproblem.

A.2 Feasibility and Optimality Cuts for CVaRS Model

Analogously to above, the CVaRS model (8) can be reformulated in the form (11)–(12) as follows

$$Z \ = \ \min \quad \sum_j f_j x_j + \sum_i \sum_j c_j \zeta_{ij} + \sum_i \sum_j \lambda d_{ij} y_{ij} + \gamma t \tag{23a}$$

$$\text{s. t.} \quad \sum_j x_j = h, \tag{23b}$$

$$y_{ij} \le x_j, \qquad \forall i, j, \tag{23c}$$

$$\zeta_{ij} \le M y_{ij}, \qquad \forall i, j, \tag{23d}$$

$$x_j, y_{ij} \in \{0,1\},\ \zeta_{ij} \in \mathbb{Z}_+,\ t \in \mathbb{R}, \tag{23e}$$

with the subproblem (20) defined as:

$$t(\hat{\mathbf{z}}) \ = \ \min \quad \eta + \frac{1}{1-\alpha} \sum_k \pi_k U_k \tag{24a}$$

$$\text{s. t.} \quad q_{ijk} \le Q_{jk}\hat{\zeta}_{ij}, \qquad \forall i, j, k, \tag{24b}$$

$$\sum_k \pi_k \sum_j q_{ijk} \ge \overline{D}_i, \qquad \forall i, \tag{24c}$$

$$w_{ik} \ge D_{ik} - \sum_j q_{ijk}, \qquad \forall i, k, \tag{24d}$$

$$U_k \ge \sum_i w_{ik} - \eta, \qquad \forall k, \tag{24e}$$

$$w_{ik}, q_{ijk}, U_k \ge 0, \qquad \forall i, j, k. \tag{24f}$$

Let α_{ijk}, μ_i, β_{ik}, and θ_k be the dual variables associated with constraints (24b), (24c), (24d) and (24e) respectively. Then, the dual of subproblem becomes

$$t(\mathbf{z}) \;=\; \max \quad \sum_i \sum_j \sum_k Q_{jk}\hat{\zeta}_{ij}\alpha_{ijk} - \sum_i \sum_k D_{ik}\beta_{ik} - \sum_i \overline{D}_i\mu_i \tag{25a}$$

$$\text{s. t.} \quad \alpha_{ijk} - \beta_{ik} - \pi_k\mu_i \le 0, \qquad \forall i, j, k, \tag{25b}$$

$$-\theta_k \le \frac{1}{1-\alpha}\pi_k, \qquad \forall k, \tag{25c}$$

$$-\beta_{ik} + \theta_k \le 0, \qquad \forall i, k, \tag{25d}$$

$$-\sum_k \theta_k \le 1, \tag{25e}$$

$$\alpha_{ijk}, \mu_i, \beta_{ik}, \theta_k \le 0, \qquad \forall i, j, k. \tag{25f}$$

If, for a given set of values $\hat{\zeta}_{ij}$, where $(\hat{x}_j, \hat{y}_{ij}, \hat{\zeta}_{ij}, \hat{t})$ is an optimal solution of (23), problem (25) is unbounded, let $(\hat{\alpha}_{ijk}, \hat{\beta}_{ik}, \hat{\mu}_i)$ be an extreme ray of the feasible region of (25), such that $\sum_i \sum_j \sum_k (Q_{jk}\hat{\alpha}_{ijk})\hat{\zeta}_{ij} - \sum_i \sum_k D_{ik}\hat{\beta}_{ik} - \sum_i \overline{D}_i\hat{\mu}_i > 0$. Then, the feasibility cut

$$\sum_i \sum_j \sum_k Q_{jk}\hat{\alpha}_{ijk}\zeta_{ij} - \sum_i \sum_k D_{ik}\hat{\beta}_{ik} - \sum_i \overline{D}_i\hat{\mu}_i \le 0, \tag{26}$$

is added to the master problem. If, on the other hand, the optimal objective $t^* = t(\hat{\mathbf{z}})$ of (25) is finite and such that $\hat{t} < t^*$, the following optimality cut is added to the master:

$$\sum_i \sum_j \sum_k Q_{jk}\hat{\alpha}_{ijk}\zeta_{ij} - \sum_i \sum_k D_{ik}\hat{\beta}_{ik} - \sum_i \overline{D}_i\hat{\mu}_i \le t, \tag{27}$$

where $(\hat{\alpha}_{ijk}, \hat{\beta}_{ik}, \hat{\mu}_i)$ is an optimal solution of (25).

A.3 Feasibility and Optimality Cuts for HMCRS Model

The polyhedral approximation of the HMCRS model (10) can be written in the form of a mixed-integer linear problem MILP where, as before, the integer-valued vector $\mathbf{z}$ comprises variables x_j, y_{ij}, and ζ_{ij}, so that the corresponding problem (11) has the form

$$Z \;=\; \min \quad \sum_j f_j x_j + \sum_i \sum_j c_j\zeta_{ij} + \sum_i \sum_j \lambda d_{ij} y_{ij} + \gamma t \tag{28a}$$

$$\text{s. t.} \quad \sum_j x_j = h, \tag{28b}$$

$$y_{ij} \le x_j, \qquad \forall i, j, \tag{28c}$$

$$\zeta_{ij} \le M y_{ij}, \qquad \forall i, j, \tag{28d}$$
$$x_j, y_{ij} \in \{0,1\},\ \zeta_{ij} \in \mathbb{Z}_+,\ t \ge 0, \tag{28e}$$

and the subproblem (12), whose optimal objective $t(\mathbf{z})$ defines the value of variable t above, takes the form

$$\begin{aligned}
t(\mathbf{z}) \;=\; \min \quad & \eta + (1-\alpha)^{-1} U_{2K-1} && (29a)\\
\text{s. t.} \quad & q_{ijk} \le Q_{jk}\zeta_{ij}, \qquad \forall i, j, n, && (29b)\\
& \sum_k \pi_k \sum_j q_{ijk} \ge \overline{D}_i, \qquad \forall i, && (29c)\\
& w_{ik} \ge D_{ik} - \sum_j q_{ijk}, \qquad \forall i, k, && (29d)\\
& U_k \ge \pi_k^{1/p}\Big(\sum_i w_{ik} - \eta\Big), \qquad \forall k, && (29e)\\
& U_{K+r} \ge a_l^{(p)} U_{2r-1} + b_l^{(p)} U_{2r}, \qquad \forall r, l, && (29f)\\
& w_{ik}, q_{ijk}, U_k \ge 0, && (29g)
\end{aligned}$$

where the nonnegative variables p_{ijk}, w_{ik}, and U_k comprise the vector $\mathbf{u}$, see (12).

Let α_{ijk}, μ_i, β_{ik}, θ_k, and ν_{lk} be the multipliers associated with constraints (29b), (29c), (29d), (29e), and (29f), respectively. Then, the dual of subproblem (29) can be written as

$$\begin{aligned}
t(\mathbf{z}) \;=\; \max \quad & \sum_i \sum_j \sum_k Q_{jk}\zeta_{ij}\alpha_{ijk} - \sum_i \sum_k D_{ik}\beta_{ik} - \sum_i \overline{D}_i \mu_i && (30a)\\
\text{s. t.} \quad & \alpha_{ijk} - \beta_{ik} - \pi_k \mu_i \le 0, \qquad \forall i, j, k, && (30b)\\
& -\beta_{ik} + \theta_k \le 0, \qquad \forall i, k, && (30c)\\
& -\sum_k \theta_k \le 1, && (30d)\\
& -\theta_k + \sum_l a_l^{(p)} \nu_{l\lceil \frac{k}{2} \rceil} \le 0, \qquad \forall k = 1, 3, \ldots, K-1, && (30e)\\
& -\theta_k + \sum_l b_l^{(p)} \nu_{l\lceil \frac{k}{2} \rceil} \le 0, \qquad \forall k = 2, 4, \ldots, K, && (30f)\\
& \sum_l A_l^{(p)} \nu_{l(\frac{K}{2}+\lceil \frac{k}{2} \rceil)} - \sum_l \nu_{lk} \le 0, \qquad \forall k = 1, 3, \ldots, K-3, && (30g)\\
& \sum_l B_l^{(p)} \nu_{l(\frac{K}{2}+\lceil \frac{k}{2} \rceil)} - \sum_l \nu_{lk} \le 0, \qquad \forall k = 2, 4, \ldots, K-2, && (30h)\\
& -\sum_l \nu_{l(K-1)} \le \frac{1}{1-\alpha}, && (30i)\\
& \alpha_{ijk}, \mu_i, \beta_{ik}, \theta_k, \nu_{lk} \le 0. && (30j)
\end{aligned}$$

For the sake of simplicity, we assume K is an even number. If, for a given optimal value $\hat{\mathbf{z}}$ obtained from (28), problem (30) is unbounded, let $(\hat{\boldsymbol{\alpha}}, \hat{\boldsymbol{\beta}}, \hat{\boldsymbol{\mu}})$ be an extreme ray of (30), such that $\sum_i \sum_j \sum_k Q_{jk}\hat{\alpha}_{ijk}\hat{\zeta}_{ij} - \sum_i \sum_k D_{ik}\hat{\beta}_{ik} - \sum_i \overline{D}_i \hat{\mu}_i > 0$. Then, a feasibility cut

$$\sum_i \sum_j \sum_k Q_{jk}\hat{\alpha}_{ijk}\zeta_{ij} - \sum_i \sum_k D_{ik}\hat{\beta}_{ik} - \sum_i \overline{D}_i \hat{\mu}_i \le 0, \tag{31}$$

is added to (28). Conversely, let $\hat{t}$ and t^* denote an optimal value of t in the master problem (28), and the optimal objective function value of problem (30), respectively. If $\hat{t} < t^*$, then an optimality cut

$$\sum_i \sum_j \sum_k Q_{jk}\hat{\alpha}_{ijk}\zeta_{ij} - \sum_i \sum_k D_{ik}\hat{\beta}_{ik} - \sum_i \overline{D}_i \hat{\mu}_i \le t, \tag{32}$$

is added to the master problem (28).